AD-A061 447 RENSSELAER POLYTECHNIC INST TROY N Y DEPT OF MATERIA--ETC F/G 11/6
ENVIRONMENTAL EFFECTS ON GENERAL FATIGUE RESISTANCE AND CRACK N--ETC(U)
NOV 78 D J DUQUETTE
N00014-75-C-0466

UNCLASSIFIED

NL

| OF |
AD
A061447

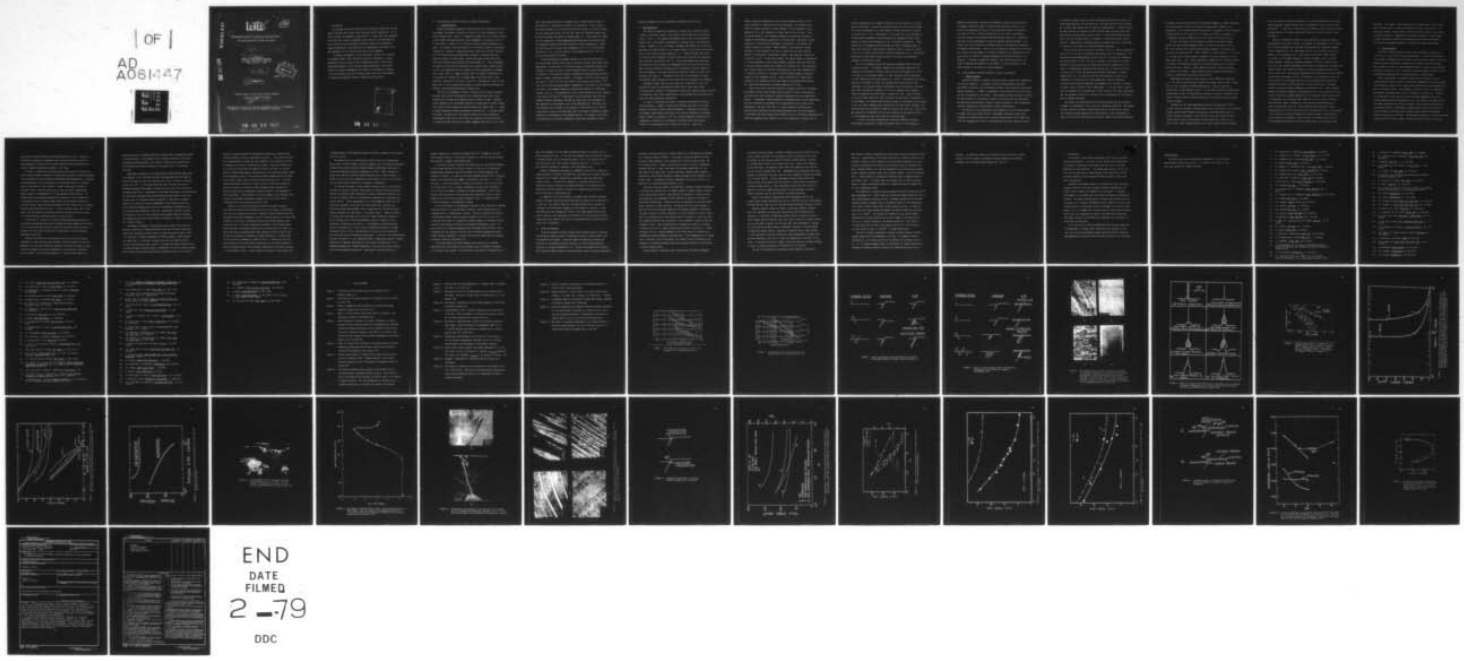

END
DATE
FILMED
2-79
DDC

LEVEL II

12

6

ENVIRONMENTAL EFFECTS ON GENERAL FATIGUE RESISTANCE AND CRACK NUCLEATION IN METALS AND ALLOYS

9 Technical rept.

10 D. J. Duquette
Materials Engineering Department
Rensselaer Polytechnic Institute
Troy, New York 12181

12 56p.

11 November 1978

Technical Report to the Office of Naval Research

Project No. 15 N00014-75-C-0466

I. Introduction

The fatigue resistance of metals can be profoundly affected by environmental reactions which affect crack initiation and/or propagation. In the case of gaseous environments, oxide films or, in some cases, gas adsorption alone have been related to premature crack initiation for some materials. Crack initiation in other materials does not appear to be affected by gaseous environments, particularly at low temperatures, and there is not good agreement on the criteria which govern these phenomena.

In aqueous environments, on the other hand, virtually all corrosive environments affect crack initiation processes, sometimes by a simple phenomenon of pits acting as stress concentrators and, at other times, through what appears to be a far more complex phenomenon. This review details the general phenomena of the affects of environment on fatigue lives and discusses some of the current models which have been proposed to explain environmental effects on fatigue crack initiation.

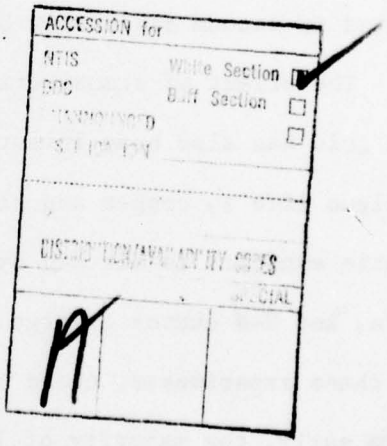

II. Environmentally Assisted Fatigue in Gaseous Environments

A. General Behavior

Gaseous environments generally reduce fatigue lives of metals and alloys. For example, experiments conducted in vacuum, or in inert atmospheres, often lead to longer lives. While it is generally assumed that the principal effects of environment are associated with crack propagation, the subject of part II of this paper, a review of a few results on smooth surfaced specimens is in order. For example, Gough and Sopwith, in an extensive series of experiments conducted on a variety of engineering alloys, noted that a partial vacuum of only 10^{-3} mm Hg resulted in appreciable increases in fatigue lives and endurance limits for carbon steels, brasses and copper, while 30% copper-nickel and chromium steels showed little improvement [1]. Later experiments on copper and 70-30 brass in laboratory air, partial vacuum, humidified and dry air, and humidified and dry nitrogen led these investigators to suggest that a joint effect of oxygen and water vapor is primarily responsible for the reduction of fatigue life, although oxygen alone also leads to some reduction, especially in the case of brass [1]. Experiments on lead [2] and Armco iron [3] also showed marked changes in fatigue behavior with materials tested in vacuum exhibiting extended fatigue lives.

The effect of atmospheric oxygen on fatigue lives in copper, aluminum, and gold has also been investigated [3-5]; oxygen and water vapor reduce fatigue life in copper and aluminum but have no effect on gold. Alternate static exposure to air and dynamic exposure to vacuum does not affect fatigue life, and S-N curves diverge as applied stresses are reduced (Fig. 1). Based on these experiments, these investigators concluded that: 1) fatigue cracks form early, the majority of life being concerned with crack propagation (environment having little or no effect on nucleation and initial growth); 2) oxygen and water vapor are the primary damaging constituents in air (water

vapor alone being effective in aluminum); and 3) oxygen must be a gas, i.e. pre-oxidation or intermittent exposure is not effective. Similar results were also obtained for an iron-0.5%-carbon alloy tested in air and in vacuum, with the significant result that air also lowers the observed fatigue limit as well as fatigue life above the fatigue limit [4]. This result was linked with the appearance of non-propagating microcracks below the fatigue limit; air apparently reducing the stress required to affect propagation. Vacuum has also been shown to delay crack propagation in Ni [6], in nickel-base superalloys [7-8], in Cu-Al alloys at room temperature and at 77°K [9], and in polycrystalline Pb [10-16].

For most materials, environment appears to be most effective early in the crack growth process, with little or no effect at high crack growth rates. Additionally, the majority of S-N curves diverge at decreasing stresses, the increase in fatigue life due to vacuum becoming greater at lower stresses. In contrast to this behavior, however, aluminum and aluminum alloys have been shown to exhibit conflicting results. For example, a 2017-T4 alloy tested in air and at 2×10^{-6} torr [17] and a 2024-T3 alloy tested in air and at 10^{-10} torr [18] in rotating bending exhibit convergence of S-N curves at low stresses, the effect of environment apparently becoming less important at decreasing stresses (Fig. 2). Pure aluminum [19] and an 1100 aluminum alloy [20] compared in air and at 10^{-6} and 10^{-7} respectively, on the other hand, show the more commonly observed divergence, and Meyn has shown that crack propagation is more sensitive to environment at low strain amplitudes in a 2024 alloy [21]. This conflict may be related to the presence of water vapor at the "softer" vacuum levels, since it has been shown that the fatigue of aluminum is highly sensitive to the presence of this gaseous species. For example, water vapor has been shown to be the only atmospheric constituent necessary to induce

enhanced propagation rates in aluminum and aluminum alloys [22-23].

B. Crack Nucleation

The effects of gaseous environments on fatigue crack initiation remain a highly controversial subject, with opinion being divided into two opposing points of view: 1) that gaseous environments play no part in the nucleation process, and 2) that gaseous atmospheres very strongly affect the nucleation process. Thompson, et al, for example, expressed the opinion that cyclically generated slip bands produced in air became regions of high oxygen concentration due to strain induced vacancy generation [5]. Dissolved oxygen then serves to prevent initial rewelding of nascent cracks and accelerates the transition from slip band to microcrack (Fig. 3). Other investigators have postulated that metal and alloy surfaces are strengthened with an oxide film, and that, when cyclically stressed, dislocations are accumulated in surface regions so that the formation of cavities and voids is enhanced, leading to early crack formation [19] (Fig. 4). According to this view, in the absence of oxygen dislocations readily escape from the surface and crack nucleation is retarded.

Atmospheric water vapor has also been cited as important to the crack nucleation process in age-hardened aluminum alloys, water vapor either accelerating the oxidation of emerging slip steps (thus blocking reverse slip)[24] or alternately, water vapor dissociating to form hydrogen which embrittles the alloy and causes premature cracking [22].

In order to investigate the effect of gaseous environments in fatigue crack nucleation, a number of authors have compared the effects of air and vacuum on cyclically induced surface deformation. Grosskreutz and Bowles, for example, showed marked reductions in the surface deformation of aluminum single crystals at pressures of 10^{-9} torr versus atmospheric pressures, and suggested an interaction of environment with newly formed slip steps to account for the suppressed slip in vacuo [25] (Fig. 5). Later work,

however, based on observations of pre-oxidized aluminum crystals ($\sim$ 50 Å Al_2O_3), resulted in a modification of this mechanism. The stripped oxide, tested in vacuum, exhibited a Young's modulus $\sim$ 4X that exhibited in air, apparently due to the elimination of water vapor in the film [26]. Thus, the reduced degree of slip intensity observed in vacuum was attributed to changes in the mechanical properties of the oxide film. The delay of crack initiation in vacuum would accordingly be attributed to the reduced slip intensity observed in vacuum. Marked changes in slip intensity between specimens of lead fatigued in air and in vacuum have also been reported. Contrary to Grosskreutz' observations, however, lead shows more rumpling in vacuum than in air. In this case, however, the reduced degree of deformation in air was attributed to early grain boundary cracking, which was sufficient to relieve surface stresses and, therefore, to inhibit slip. The observation that fatigue cracks are initiated intergranularly in air and transgranularly in vacuum was related to a reduction of grain boundary energy by adsorbed oxygen from the atmosphere [15,29]. Similar observations of reduced slip intensity in the presence of thin oxide films in vacuum have been observed for nickel-base superalloys at elevated temperatures [27,28].

While little effort has been directed at studying the effects of gaseous environment on high strain fatigue crack initiation, several investigations have shown that oxide produced at elevated temperatures can have significant effects. Intergranular crack nucleation in stainless steels at high temperatures has been attributed to the effect of an oxide-induced notch created during preheating of the alloy [30] (Fig. 6). Oxide cracking in preferentially oxidized grain boundaries of nickel base superalloys has also been suggested to accelerate low cycle fatigue crack initiation in air at elevated temperatures [31]. Coffin has suggested that virtually all of the degradation in fatigue life at

elevated temperatures of a number of materials can be attributed to environmental interactions, noting that frequency effects in the low cycle fatigue law could be eliminated for a large number of metals and alloys by testing in vacuum (Fig. 7) [32]. Additionally, it was noted that tests performed in vacuum showed transgranular crack nucleation and propagation versus intergranular nucleation and propagation in air at elevated temperatures. These results are not unambiguous since Koburger has shown a frequency effect in high cycle fatigue for directionally solidified eutectic alloys when tested in air and in vacuum, particularly at elevated temperatures [33]. The primary difference in these results may be related to the lack of intergranular cracking in the eutectic alloys.

Not all investigators agree that gaseous environments affect the crack nucleation process. For example, Wadsworth and Hutchings showed that the appearance of intrusions, extrusions and microcracks was similar in air and in vacuum for an equivalent number of cycles, although further development of these features was very much reduced [3]. Hordon, investigating the fatigue behavior of aluminum in vacuum, has expressed the opinion that not only initiation, but the entire Stage I propagation step is unaffected by environment, while adsorption of oxygen at the tip of a growing crack increases Stage II propagation and thus reduces fatigue life [20]. Laird and Smith, on the other hand, agree that crack initiation in pure metals is unaffected by environment, but observed that the early stages of crack growth are increased by air, the effect becoming less pronounced as the crack growth proceeds: [34] they attributed this increase to chemical attack of the crack tip. Achter [35], and Latanision and Westwood [36] have also related the environmental effect to the propagation stage rather than the initiation stage.

In view of the rapid contamination of metallic surfaces by gaseous environmental adsorbates, critical experiments remain to be performed to

understand the effects of gaseous environments on fatigue crack nucleation. For example, monolayer oxygen coverage of newly generated surfaces in air occurs in microseconds and even if a relatively good vacuum is obtained (of the order 10^{-6} torr), surface coverage will occur in only a few seconds. Since the fatigue crack initiation process has been shown to be a relatively slow step involving thousands of cycles at moderate applied stresses, it is evident that crack initiation in practice rarely occurs without an oxidizing environment being present. While it may be possible to examine crack initiation as a function of environment if ultrasonic frequencies are combined with ultra high vacuum, the effects of gaseous atmospheres on nucleation remain to be resolved. It should be emphasized, however, that from available data, the effect of gaseous environments (if one exists) on crack nucleation is very small compared to the effect on crack propagation.

III. Environmentally Assisted Fatigue in Aqueous Environments

A. General Behavior

Important variables in aqueous corrosion fatigue include alloy composition and solution chemistry. In general, corrosion fatigue behavior parallels environment corrosivity, with increasing corrosion rates resulting in decreased fatigue resistance. A number of exceptions to this observation have been noted and will be discussed in this paper. (When improved corrosion fatigue resistance has been observed to be inversely related to corrosion rate, the improvement has generally been ascribed to delays in crack initiation or early propagation caused by dissolution of microcracks or stress concentrators.)

The effects of salt concentration and temperature on the fatigue behavior of steels have been studied [37-41]. Experiments performed on mild steel specimens in distilled water and in various concentrations of KCl showed that solutions ranging from 2 molal to 1/40 molal have virtually identical effects

on corrosion fatigue lives, but that at concentrations below 1/40 molal, the effect approached that of distilled water, although corrosion rates increase in an almost linear manner with solution ion concenteration. A similar result has been reported for deaerated 3% NaCl solution where corrosion rates were controlled by applied anodic currents (Fig. 8). These observations indicate that a critical corrosion rate is a necessity to initiate corrosion fatigue failures. Additionally, increasing overall corrosion rates over a long range of rates has little effect on corrosion fatigue resistance.

Tests on mild steel in artificial sea water [38] in a constant temperature room at 15, 25, 35 and 45°C showed an appreciable effect of temperature, with fatigue life being approximately halved in the 10^7 cycle when the temperature was raised from 15 to 35°C. This is in contrast to the normal air fatigue behavior of steel which shows no appreciable effect of temperature in this range. At temperatures approaching the boiling point of water (82°C), drill rod tested in 2.5% NaCl solutions showed definite improvement at higher temperatures [41]. The authors attributed this beneficial effect to the difference in pitting attack at high temperature, the pits being more uniformly distributed and shallower, and suggested that the ratio of cathodic to anodic areas is higher at lower temperatures. It is more likely, however, that the decrease in O_2 concentration of the solution at the higher temperature and the subsequent reduction in corrosion rate is responsible for the improvement in fatigue resistance.

The effect of stress frequency on corrosion fatigue has been studied by a number of investigators, but is still not completely understood. For example, an early review of corrosion fatigue noted that it is difficult to compare the corrosion fatigue properties of metals exposed to like environments in view of the fact that data reported are usually taken at different frequencies.

In general, a given time was found to produce more damage at a higher frequency, but a given number of cycles was found to produce greater damage at low frequencies. For low alloy steels in fresh water, a frequency of 1450 cycles/min produced failure in 10^6 cycles or 11 1/2 hours, but that at a frequency of 5 cycles/min, failure occurred in 0.11×10^6 cycles or 400 hours [43,44].

To date, the effect of pH of aqueous solutions on corrosion fatigue behavior has not received extensive study. A study of the effect of 0.1N HCl on the fatigue life of steels showed greater damage in this medium than in neutral KCl solutions [45]. Tests conducted in alkaline media, at a pH above 12.1, showed that a fatigue limit is regained, this limit improving at still higher pH's (Fig.)[46]. These investigators suggested that corrosion fatigue is a result of differential aeration cells which produce pits in the metal surface and that a high pH provides diffusion barriers (ferrous hydroxide) to oxygen on the surface. Higher fatigue limits at high pH are explained in terms of a "better and more perfect film barrier".

Experiments performed on boiler steels at 275°C showed that additions of 0.7 g/l NaOH to distilled water improved the fatigue limit by approximately 20%, but that increasing the NaOH concentration to 200 g/l lowered the fatigue limit by approximately 10% [47]. At the higher alkaline concentrations, intergranular as well as transgranular cracking was observed, indicating that caustic cracking (stress corrosion cracking) was also occurring during normal fatigue cracking.

Although in a few cases annealing was shown to be beneficial [48,49], alloying and heat treatment of steels usually have little effect on the corrosion fatigue characteristics unless the alloying is undertaken specifically to improve corrosion resistance. Thus, the use of low alloy steels and high carbon steels in most corrosive media is only beneficial in that, in air, their fatigue limit increases directly with their ultimate tensile strengths.

It is not possible to predict the effects of a given environment for all alloys since subsequent fatigue resistance will be dependent on such factors as notch sensitivity. In some cases, deleterious heat treatments such as those which lead to sensitization in stainless steels have resulted in lower corrosion fatigue resistance.

There is considerable evidence for the importance of dissolved oxygen to the mechanism of corrosion fatigue. For example, an improvement in the fatigue life of steel specimens was noted when the specimens were completely immersed at 96°C, suggesting that this improvement was due to the limited solubility of oxygen at this temperature [50]. Sodium chloride solution dripped through air proved to be extremely damaging to fatigue specimens, while a solution dripped through a commercial hydrogen atmosphere resulted in higher fatigue life, with still further improvement as the purity of hydrogen was increased [51]. Similar effects were observed on steels in aerated and deaerated steam and on lead in acetic acid (investigators hypothesized that hydrogen evolution shielded the specimen from oxygen) [52,53]. The effects of air, hydrogen sulfide, and carbon dioxide on the fatigue behavior of both normalized and quenched and tempered 1035 steel in 5% NaCl solution [54] have been studied. Hydrogen sulfide was not particularly damaging in the absence of air. Carbon dioxide, however, was equally damaging in the presence of air. More importantly, these results showed that complete deaeration of the sodium chloride solution caused a re-appearance of the fatigue limit observed in dry air tests, indicating that dissolved oxygen is essential to the corrosion fatigue mechanism in neutral pH solutions (Fig. 10). This result was also confirmed by other investigators for 3% NaCl solutions and for distilled water [55]. The presence of the chloride ion alone in deaerated solutions, however, is sufficient to lower fatigue life although it does not affect the fatigue limit (Fig. 11). Electrochemical polarization may have a marked effect on corrosion fatigue

resistance. For example, anodic polarization of carbon steels and of copper alloys has been shown to result in decreases in fatigue lives [55-57]. For some cases, however, severe anodic polarization actually results in increases in fatigue resistance. Examination of specimens subjected to large amounts of anodic dissolution reveals that surface initiated cracks are blunted by the corrosive environment, leading to a decrease in stress concentration.

B. Crack Nucleation

Theories of aqueous corrosion fatigue crack nucleation have generally relied on one or more of the following mechanisms: 1) stress concentrations at the bases of hemispherical pits created by the corrosive medium, 2) electrochemical attack at plastically deformed areas of metal, with non-deformed metal acting as cathode, 3) electrochemical attack at ruptures in an otherwise protective surface film, and 4) lowering of surface energy of the metal due to environmental adsorption and increased propagation of microcracks.

Early investigators of corrosion fatigue [58,59] favored the stress-concentration pit theory, based on the physical examination of failed specimens which revealed a number of very large cracks originating at large hemispherical pits at the metal surface. Pit formation in metals and alloys in aggressive environments undoubtedly does lead to a reduction in fatigue life. However, it is important to note that the corrosion fatigue phenomenon also occurs in environments where pitting does not occur. For example, low carbon steels are highly susceptible to corrosion fatigue in acid solutions where pits are not observed [60,61]. Additionally, reduced fatigue lives can be induced in steel specimens by the application of small anodic currents in deaerated solutions where pits do not form. Fatigue tests performed in 3 percent NaCl+NaOH solution of pH 12, where a number of randomly distributed pits are observed,

show fatigue limits identical with those observed in air [42]. Results of this kind are perhaps not unexpected since corrosion induced pits tend to be hemispherical in nature and the stress intensity factor associated with surface connected hemispherical defects is not large.

In order to examine the corrosion fatigue crack initiation process, low carbon steels fatigued in neutral 3 percent NaCl solutions for small percentages of total fatigue life were sectioned and examined metallographically. Although some hemispherical pits were observed in the specimen surface, no cracking could be attributed to their presence. Rather, accelerated corrosion of initiated stage I cracks was noted, with a deep "pit-like" configuration being oriented at approximately 45° to the specimen surface (Fig.11). No fatigue cracks were observed emanating from these pits, and an examination of specimens cycled for longer periods showed that the extent of growth of initiated fatigue cracks was always equivalent to "pit" depth, with no "normal" fatigue cracks associated with pits. It may be concluded then, that in many cases, the pits observed at failure by previous observers are not the cause of corrosion fatigue cracking but rather the result [55].

On the basis of a series of corrosion fatigue experiments performed on cold worked and annealed steel wires, Whitwham and Evans suggested that failure is due to distorted metal acting as anode with undistorted metal acting as cathode; very fine cracks advancing by a combination of electro-chemical-mechanical action [62].

Surface film rupture as the principal cause of the corrosion fatigue phenomenon of steels has been also proposed. Evans and Simnad [45,61] also suggested that film rupture might be important in neutral solutions but that structural changes in the metal predominate in acid solutions (distorted metal as anode). The electrode potential of a steel has been observed to

become more active in fatigue tests with a higher rate of change being noted at higher stresses. This potential drop continues throughout a particular alternating stress experiment, but reaches a steady-state in static tests. This observation has been attributed to the destruction of a protective film [63].

Experiments conducted on low carbon steels in chloride have shown that there appears to be a critical corrosion rate associated with the onset of corrosion fatigue and that this corrosion rate is not a function of applied stress level [42]. (It has been shown that this "critical" rate has no fundamental meaning since general corrosion does not occur over the entire specimen surface [64].) Additionally it was shown that steels could effectively be cathodically protected from corrosion fatigue either above or below the fatigue limit at a potential which corresponds to that which is normally observed for cathodic protection independent of the applied stress level. This observation suggests that there is no fundamental thermodynamic shift in the equilibrium potential of the iron. Additionally corrosion fatigue was observed to occur in acid solutions where adherent films are unstable, thus suggesting that film rupture cannot be accepted as a general mechanism for corrosion fatigue.

Experiments performed on polycrystalline pure copper (which does not exhibit a reduction in fatigue resistance under free corrosion conditions) showed that increasing corrosion rates, by applying anodic currents, result in a reduction of fatigue resistance in a similar manner to that observed for steels [56]. A "critical" corrosion rate also was observed (Fig.12). (At very high corrosion rates, there is a reversal in fatigue resistance due to rapid blunting of nascent cracks.) Examination of the free surfaces showed that, while slip band crack initiation was observed in air, free corrosion

resulted in mixed transgranular-intergranular cracking and applied anodic currents resulted in totally intergranular failures. Slip bands were shown to be preferentially corroded and there appeared to be an increase in both the magnitude and density of emerging slip bands. These data indicate that it is the local rather than the general corrosion rate which is critical. Figure 13 shows metallographic cross-sections of the copper and clearly shows the intergranular nature of the corrosion fatigue cracking and the increase in slip offset height under corrosion fatigue conditions [57]. Corrosion fatigue experiments conducted on single crystals of identical orientation showed an increase in corrosion fatigue resistance under conditions of applied current and an approximately twofold increase in the magnitude of slip step offsets. The character of the slip offsets is also affected, with clusters of persistent slip bands occurring in air and a more uniform distribution of active dissolution (Fig.14) [64].

Analysis of the results obtained for steels and copper indicates that corrosion fatigue crack initiation occurs by two steps; (a) persistent slip bands are preferentially attacked leading to stress intensification and subsequent early crack propagation, and (b) corrosion results in a significant increase in the density of persistent bands which produce numerous crack initiation sites. The latter observation presumably occurs because metal atoms associated with mobile dislocations in the persistent slip bands are more active than surrounding metal atoms, leading to strain relief in the surface and significant increases in surface deformation. A simple model of this process is schematically shown in Fig. 15. Rollins and Pyle have also observed active current spikes associated with slip band emergence in passive stainless steels, with subsequent repassivation occurring if strain is held constant [65,66]. Current spikes are observed in both tension and

compression modes of deformation, although the effect is greater in the tensile half of the cycle.

The observation that polycrystalline copper fails in an intergranular manner under corrosion fatigue conditions suggests that the enhanced deformation associated with grain boundaries causes enhanced preferential dissolution of the grain boundaries relative to emerging slip bands. Single crystals of copper show improved corrosion fatigue resistance due to crack blunting. In steels, on the other hand, preferential grain boundary attack is not observed and corrosion fatigue failures are accordingly transgranular.

The fatigue resistance of high strength aluminum alloys is also severely affected by corrosive solutions, particularly in chloride solutions, and this behavior has generally been attributed to either preferential dissolution at the tips of growing cracks or to preferential adsorption of a damaging ionic species [66-69]. Recent experiments on a 7075-T6 commercial alloy and on a high purity analogue of the alloy (Al-5.0Zn-2.5Mg-1.5Cu) indicate that localized hydrogen embrittlement may be responsible for the poor corrosion fatigue resistance of these alloys. For example, Fig. 16 shows the results of fatigue tests performed on the 7075 alloy under simultaneous exposure to cyclic stresses and a corrosive environment (curve B) compared to tests performed in laboratory air (curve A). If specimens are pre-corroded and tested in laboratory air, there is also a significant reduction in fatigue resistance (curve C) [70]. The reduction in life at low N_f is associated with pits which form at non-metallic inclusions. If the alloy is re-solutionized and aged, equivalent to a low temperature bake, a significant amount of fatigue resistance is regained, indicating at least partial reversibility of the damaging phenomenon and strongly suggesting a solid solution effect arising from the environmental interaction. Additionally, the reversibility in

fatigue resistance is a function of baking time [70]. Hydrogen is the only stable gaseous species at the corrosion potential of the alloy and gas bubbles were observed to emanate from growing cracks.

It had been previously observed that halide ions are particularly damaging to the fatigue behavior of Al alloys, however, if the alloy is cathodically charged during stressing, sulfate ion proves to be equally damaging, particularly at long N_f. At lower N_f the slight decrease observed in Cl^- solutions appears to be associated with damage to the passive film (Fig.17). In $SO_4^=$ solutions, a crack must initiate to break the protective film to allow access to the bulk alloy [71,72]. Cathodic charging of the high purity analogue of the 7075 alloy also shows a reduction in fatigue resistance. In many cases, fatigue crack initiation in the equi-axed grain high purity alloy is intergranular, and at more active cathodic potentials there is a tendency toward a higher percentage of transgranular cracking.

The relative amount of intergranular cracking is also a function of applied stress levels and, for the most active condition, lower stresses lead to an increased amount of intergranular cracking. This data indicates that there is a relationship between stress corrosion cracking of the alloy and corrosion fatigue, and that there is a competition between transport of hydrogen to grain boundaries and hydrogen interacting with growing transgranular cracks. At long lives or for rapidly propagating cracks hydrogen cannot diffuse to grain boundaries and thus interacts with the tips of growing transgranular cracks. Stress corrosion cracking of a similar alloy has been associated with hydrogen cracking by Swann and co-workers [73].

It has been argued that bulk aluminum alloys should not be hydrogen embrittled since the solubility and diffusion rates of hydrogen in aluminum are relatively low, however, the sub-critical crack growth in aluminum alloys

need only propagate into the region immediately ahead of a growing crack to affect propagation rates. It has also been suggested that accelerated transport of hydrogen might occur by dislocation motion [74,75], and tensile tests of the high purity alloy under cathodic charging conditions in 1N H_2SO_4 + As show serrated yielding in contrast to tests performed in air.

Finally, experiments performed on a commercial 7075 alloy in a mode III loading condition (torsion), indicated that the reduction in fatigue resistance associated with cathodic charging was considerably less than under mode I loading (Fig.18). Although total immunity to corrosion fatigue was not observed, the slight reduction in fatigue resistance can be associated with conditions which did produce a true mode III loading condition both on a micro-scale and on a macro-scale [76].

To summarize the Al alloy results, it appears that corrosion reactions liberate hydrogen, which effectively embrittles the region in the vicinity of a crack tip. The specific details of the embrittlement are not known, but it appears that dislocation transport of the hydrogen is involved. It has been speculated that hydrogen may collect at the semi-coherent precipitate-matrix interface, thus explaining the reported (100) fracture plane, however, a great deal more research will have to be performed before a more definitive answer will be available.

IV. Protective Measures

Protection against corrosion fatigue crack initiation which is affected by environment consists chiefly of isolating the metal or alloy surface from the aggressive environment. Thus both organic and inorganic coatings are effective as are chemical reaction coatings, the latter being especially important at elevated temperatures [77]. Several investigators have reported some protection against aqueous corrosion fatigue either by inducing compressive

stresses at the metal surface, by adding inhibitors to the aqueous environments, or by applying external currents. For example, protection against corrosion fatigue has been obtained by shot peening [78], surface rolling [79,80], and by nitriding [81,82]. However, the protective action of surface compression, although effective in short time tests, may decrease considerably in long time tests in sea water [83]. On the other hand, nitrided steels showed no rusting and a 500 to 800% increase in fatigue strength without showing a true fatigue limit. Nitriding and surface compression have also been shown to be beneficial for improving fatigue behavior in air.

Inhibitors have been shown to be beneficial, although a higher concentration of inhibitor was required than is normally needed to prevent uniform corrosion in the same solution [83-86]. More inhibitor is required at higher chloride concentrations, and dichromate of 200 to 800 ppm is superior to chromate of equivalent concentration. Crevice corrosion was observed at a solution-rubber washer interface in these solutions. Saturation with zinc yellow pigment is more effective than equivalent additions of potassium chromate in preventing corrosion fatigue in chloride solutions, but as the inhibitor is added, results tend to be scattered and no true fatigue limit is obtained for long time tests. This anomalous behavior was attributed to local breakdown of passive films and subsequent attack. High concentrations of chromate are required to initiate a passive film, but the lower concentrations sufficed to maintain it. Sodium carbonate [37] and trisodium phosphate [47,87] were shown to be effective in preventing corrosion fatigue in distilled water. The re-appearance of a fatigue limit in solution of pH 12 and greater can probably also be attributed to the presence of a protective passive layer which reduces corrosion to a rate below a certain critical value.

Various cathodic, anodic, and inert coatings have also been investigated

to prevent corrosion fatigue. Cathodic coatings can only be effective if the coating remains unbroken, and accordingly several investigators have shown that breaks in the coating accelerate corrosion fatigue behavior, probably by accelerating corrosion at the breaks (Fig. 19a). Anodic metal coatings, on the other hand, have generally been shown to be beneficial even when the film was locally ruptured (Fig. 19b). Experiments with galvanized steel wires provided an indication that zinc could be used to markedly increase the fatigue life of steels [88,89]. Further experiments confirmed these results and indicated that electroplated zinc was superior to galvanizing in preventing corrosion fatigue [90,91]. Other investigators [80,92-94] have studied the behavior of zinc and cadmium electroplates on steel specimens in various aqueous solutions, and all have arrived at the same conclusion.

Organic and inorganic coatings have been investigated and the only purpose these coatings apparently serve is as a physical barrier to surrounding solutions and that they were not effective unless absolutely continuous [95,96].

Applying cathodic current as a means of reducing corrosion fatigue of steel wire specimens in neutral KCl solutions has been investigated [61]. Although it is possible to completely prevent failure in these solutions, a lower fatigue limit is observed, this limit being a function of applied current. In acid solutions (0.1N HCl), on the other hand, some improvement of fatigue life with applied cathodic current is observed, although it is not possible to completely inhibit failure. Analyses of dissolved iron at high currents (2 ma) indicated no corrosive attack, but these investigators concluded that any iron dissolved at the tip of a crack was redeposited at the mouth of the crack. It was also noted that a higher current was required at higher stresses in order to prevent accumulation of dissolved iron in solution.

The use of potentiostatic polarization allows complete protection of

mild steels by cathodic polarization in both neutral and acid solutions [42,55] (Fig. 20). Significantly, the critical potential for complete protection from corrosion fatigue is nearly identical to the calculated potential of an iron surface in equilibrium with ferrous ion in solution below the fatigue limit. Thus a potential where no Fe ions are dissolved in the solution (no corrosion occurs) completely protects steel from corrosion fatigue. In low pH solutions (pH 2), copious amounts of hydrogen are liberated with no apparent effect on the fatigue limit. At stresses above the fatigue limit in these solutions, however, cathodic polarization results in a marked increase in fatigue life--an as yet unexplained result.

The possibility of anodic protection against corrosion fatigue has also been investigated for a 0.48% C steel in an acetate buffered solution of pH 4.6 under potentiostatic conditions [97,98]. Although fatigue life of the steel remained constant throughout most of the passive region of the polarization curve (+200 to +900 mv versus SCE), failure always occurred. It should be noted that the current observed throughout the passive region was relatively high (3 to 4 ma/cm^2). The fatigue life observed at this current agreed qualitatively with that observed in the active region of the polarization curve, e.g., failure occurred in the passive region in 5×10^5 cycles at a stress level equal to 90% of the fatigue limit and in 4×10^5 cycles at an active anodic current of 3 ma/cm^2 at the same stress level.

The use of cathodic protection to prevent corrosion fatigue of steels depends sensitively on the hardness of the stee. For example, cathodic protection of a 4140 steel was shown to be feasible for hardness values of R_c 40. At higher hardness values, an improvement in fatigue resistance is observed for moderate cathodic potentials but complete protection is not

possible. At potentials which are sufficiently large to inhibit corrosion fatigue for softer steels, a decrease in fatigue resistance is observed, presumably due to hydrogen embrittlement [99] (Fig. 20).

V. Conclusions

On the basis of the evidence presented in this review, two major points become apparent. The first is that fatigue crack initiation in the presence of aggressive environments does not occur by the same mechanism for every material. The second point is that, for all the work that has been done to define fatigue crack initiation, no model has been presented for any system which does not have at least a few major discrepancies.

Aggressive environments appear to accelerate the crack initiation process, although in the case of gases at ambient temperatures, the effect on total fatigue life appears to be very small. In aqueous environments, on the other hand, the initiation process is dramatically affected. Previously proposed models to explain this behavior have not accounted for all reported experimental detail, especially the fact that fatigue behavior is seriously affected at extremely low corrosion rates. However, if it is assumed that corrosion need only take place at specific areas, such as at emerging slip bands, a new model may be sustained. This model is based on accelerated slip connected with the removal of dislocation locking sites.

As a final note, it should be emphasized that the exact mechanism (or mechanisms) of fatigue crack initiation in the presence of both inert and corrosive environments remains elusive, and rather elaborate experimentation is required before satisfactory models can be developed.

ACKNOWLEDGEMENT

The author would like to express his appreciation to the Office of Naval Research and particularly Dr. P. A. Clarkin, for support of this work under Contract No. N00014-75-C-0466.

1. H.J. Gough and D.G. Sopwith, J. Inst. Metals, 72, 415(1946).

2. H. J. Gough and D.G. Sopwith, J. Inst. Metals, 52, 55 (1935).

3. N.J. Wadsworth and J. Hutchings, Phil. Mag., 3, 1154(1958).

4. N.J. Wadsworth, Phil. Mag. 6, 387(1961).

5. N. Thompson, N.J. Wadsworth and N. Louat, Phil. Mag 1, 113(1956).

6. R.L. Stegman and M. Achter, Trans. TMS-AIME 239, 742(1967).

7. D.J. Duquette and M. Gell, Met. Trans. 2, 1325(1971).

8. H.H. Smith and P. Shahinian, Trans. ASM 62, 549(1969).

9. C.Laird and A.R. Krause, Trans. TMS-AIME 242, 2339(1968).

10. K.U. Snowden, Phil. Mag. 3, 1411(1958).

11. K.U. Snowden and J.N. Greenwood, Trans. TMS-AIME 212, 91 (1958).

12. K.U. Snowden and J.N. Greenwood, Trans. TMS-AIME 212, 627 (1958).

13. K.U. Snowden, Phil. Mag. 6, 321(1960).

14. K.U. Snowden, Nature (London) 189, 53(1961).

15. K.U. Snowden, Acta Met. 12, 295(1964).

16. K.U. Snowden, Phil. Mag. 10, 435(1964).

17. J.M. Jacisin, Trans. TMS-AIME 239, 821(1967).

18. W. Engelmaier, Trans. TMS-AIME 242, 1713(1968).

19. H. Shen, S.E. Podlaseck and I.R. Kramer, Acta Met. 14, 341 (1966).

20. M.J. Hordon, Acta. Met. 14, 1173(1966).

21. D.A. Meyn, Trans. ASM 61, 53(1968).

22. T. Broom and A. Nicholson, J. Inst. Met. 89, 183(1960).

23. F.J. Bradshaw and C. Wheeler, Mat. Res. 2, 112(1966).

24. J.A. Bennett, J. Res. NBS, 68C, 91(1964).

25. J.C. Grosskreutz and C.Q. Bowles, Environment Sensitive Mechanical Behavior, Eds. Westwood and Stoloff, Gordon and Breach (1967).

26. J.C. Grosskreutz, Surface Sci., 8, 173(1967).

27. D.J. Duquette and M. Gell, AMRDL, Pratt and Whitney Aircraft, Middletown, Conn., unpublished research (1970).

28. H. Smith and P. Shahinian, Trans. ASM. 62, 549(1969).

29. K.U. Snowden and J.N. Greenwood, Trans. TMS, AIME, 212, 626(1958).

30. B. Hodgson, Met. Sci. J., 2, 235(1968).

31. C.J. McMahon and L.F. Coffin, Jr., Met. Trans., 1, 3443 (1960).

32. L.F. Coffin, Jr., Met. Trans. 3, 1777(1972).

33. C. Koburger, Ph.D. Dissertation, Rensselaer Polytechnic Institute, September 1978.

34. C. Laird and G.C. Smith, Phil. Mag., 8 1945(1963).

35. M. Achter, ASTM STP, 415, 181(1967).

36. R.M. Latanision and A.R.C. Westwood, Advances in Corrosion Science and Technology, p. 80, Plenum Press (1967).

37. A.J. Gould, Engineering, 136, 453(1933).

38. A.J. Gould, Engineering, 141, 495 (1936).

39. D.J. McAdam, Jr., Proc. Amer. Soc. Test. Mat., 31, 259(1931).

40. D.J. McAdam, Jr., Proc. Amer. Soc. Test. Mat., 28, 117(1928).

41. I. Cornet and S. Golan, Corrosion, 15, 262t(1959).

42. D.J. Duquette and H.H. Uhlig, Trans. ASM, 62, 839(1969).

43. M. Vater and M. Henn, Korrosion u. Metallschutz, 20, 179 (1944).

44. K. Endo and Y. Miyas, Bull. Japan Soc. Mech. Eng., 1, 374 (1958).

45. M.T. Simnad and U.R. Evans, J. Iron Steel Inst., 156, 531 (1947).

46. F.J. Radd, L.H. Crowder, and L.H. Wolfe, Corrosion, 16, 415t(1960).

47. A. Thum and C. Holzhauer, Warmë, 56 640(1933).

48. D.J. McAdam, Jr., Trans. Amer. Soc. Mech. Eng., 51, 45 (1929).

49. R. Mailänder, Krupp. Monatsh., 13, 56(1932).

50. G.D. Lehmann, Engineering, 122, 807(1926).

51. A.M. Binnie, Engineering, 128, 190(1929).

52. T.S. Fuller, Trans. Am. Inst. Min. Met. Eng., 90, 280(1930).

53. B.P. Haigh and B. Jones, J. Inst. Metals, 43, 271(1930).

54. P. Mehdizadeh, R.L. McGlasson, and J.E. Landers, Corrosion, 22, 325(1966).

55. D.J. Duquette and H.H. Uhlig, Trans. ASM, 61, 449(1968).

56. H. Masuda and D.J. Duquette, Met. Trans., 6A, 87(1975).

57. H.N. Hahn, Ph.D. Dissertation, Rensselaer Polytechnic Institute, Troy, N.Y. (1977).

58. D.J. McAdam, Jr. and G.W. Geil, Proc. Am. Soc. Test. Mat., 41, 696 (1941).

59. B.B. Westcott, Mech. Eng. 60, 813, 829(1938).

60. H. Spähn, Metalloberflache, 16, 299(1962).

61. M.T. Simnad and U.R. Evans, Proc. Roy Soc., A188, 372 (1947).

62. D. Whitwham and U.R. Evans, J. Iron and Steel Inst., 165, 72(1950).

63. A.V. Ryabchenkov, Zhur. Fiz. Khim., 26, 542(1952).

64. H.N. Hahn and D.J. Duquette, Acta Met., 26, 279(1978).

65. V. Rollins and T. Pyle, Nature 254, 322(1975).

66. T. Pyle, V. Rollins and D. Howard, J. Electrochem. Soc., 122, 1445 (1975).

67. R.E. Stoltz and R.M. Pelloux, Met. Trans., 3, 2433 (1972).

68. R.M. Pelloux, Fracture 1969, Proc. Int. Conf. on Fracture, Brighton, Chapman and Hall, 1969.

69. R.J. Selines and R.M. Pelloux, Met. Trans., 3, 2525 (1972).

70. E.F. Smith, III, R. Jacko and D.J. Duquette, Effect of Hydrogen on Behavior of Materials, Ed. A.W. Thompson and I.M. Bernstein, AIME, 1976, p. 218.

71. R.J. Jacko and D.J. Duquette, submitted to Met. Trans., 1977.

72. E.F. Smith, III, R.J. Jacko and D.J. Duquetts, Proc. 2nd Int. Congress on Hydrogen in Metals, Paris, 1977, paper 3C1.

73. L. Montgrain and P.R. Swann, Hydrogen in Metals, Ed. I.M. Bernstein and A.W. Thompson, ASM, Metals Park, 1974, p. 575.

74. J.K. Tien, Effects of Hydrogen on Behavior of Materials, Ed. A.W. Thompson and I.M. Bernstein, ASM, Metals Park, 1974, p. 207.

75. H.H. Johnson and J.P. Hirth, Met. Trans., 7A, 1543 (1976).

76. R.J. Jacko, Ph.D. Dissertation, Rensselaer Polytechnic Institute, Troy, N.Y., August 1978.

77. M. Gell and D.J. Duquette, Proc. Int. Conf. on Corr. Fat., Storrs, Conn, 1971, NACE, Houston.

78. A.J. Gould and U.R. Evans, J. Iron and Steel Inst., 156, 531 (1947).

79. A. Thum and H. Ochs, Korrosion u.Metallshütz., 13, 380 (1937).

80. O. Foppel, O. Behrens, and T. Dusold, Z. Metallkunde, 25, 279 (1933).

81. N. Inglis and G.F. Lake, Trans. Faraday Soc., 27, 803(1931); 28, 715(1932).

82. A. Jünger, Mitt. Forsch. Anstalt, Gutehoffnungshütte Oberhausen A.G., 5, 1 (1937).

83. F.N. Speller, I.B. McCorkle, and P.F. Mumma, Proc. Amer. Soc. Test. Mat., 28, 159(1928).

84. F.N. Speller, I.B. McCorkle, and P.F. Mumma, Proc. Amer. Soc. Test. Mat., 29, 239 (1929).

85. K. Daeves, E. Kamp, and K. Holthaus, Z.V.d.I., 78, 1065 (1934).

86. A.J. Gould and U.R. Evans, Iron Steel Inst. Spec. Rep., 24, 325(1939).

87. C. Holtzhauer, Mitt. Materialprüf Anst. Techn. Hochscule Darmstadt, 3(1953).

88. B.P. Haigh, Trans. Inst. Chem. Eng., 7, 29(1929).

89. B.P. Haigh and T.S. Robertson, Engineering, 138, 140(1934).

90. W.E. Harvey, Metals and Alloys, 1, 458(1930).

91. O. Behrens, Mitt. Wöhler-Inst., 15(1933).

92. N. Stuart and U.R. Evans, J. Iron Steel Inst., 147, 131(1943).

93. A. Thum and H. Ochs, Korrosion u. Metallshütz, 13, 380(1937).

94. H.J. Gough and D.G. Sopwith, J. Iron and Steel Inst., 72, 415 (1946).

95. H.J. Gough and D.G. Sopwith, J. Iron and Steel Inst., 135, 315(1937).

96. R.C. McMaster, Proc. Am. Soc. Test. Mat., 48, 628(1948).

97. H. Spähn, Metalloberfläche, 16, 369 (1962).

98. H. Spähn, Metalloberfläche, 16, 335 (1962); 16, 197 (1962); 16, 233 (1962); 16, 267 (1962).

99. H.H. Lee and H.H. Uhlig, Met. Trans., 3, 2949 (1972).

LIST OF FIGURES

Figure 8 (cont'd) stress effect and the reappearance of a fatigue limit at currents less than $\sim$ 0.2 $\mu A/cm^2$ [42].

Figure 9. The effect of pH on the fatigue behavior of low carbon steel in NaCl+NaOH. Note that a fatigue limit is observed at pH 12.1 and greater [46].

Figure 10. The effect of dissolved O_2 on the fatigue behavior of 1035 steel in 5% NaCl solution [54].

Figure 11. Crystallographic "pits" (actually trenches in low carbon steel) in 3% NaCl. Note the change of orientation from grain to grain, but the same orientation in single grains [55].

Figure 12. The effect of applied anodic current on the fatigue behavior of OFHC copper. Note the fatigue life independent region up to $\sim$ 10 $\mu A/cm^2$ and also the increase in fatigue life at currents greater than $\sim 10^3$ $\mu A/cm^2$ [56].

Figure 13. Longitudinal metallographic cross sections of Cu fatigued in (a) air showing transgranular cracking, and (b) in 0.5N NaCl showing mixed, but predominantly intergranular cracking.

Figure 14. Copper single crystal surface slip offset appearance in (a) air, 10^5 cycles, (b) air, 10^6 cycles, (c) 0.5N NaCl, $i_{applied}=100\mu A/cm^2$, 10^5 cycles, (d) 0.5N NaCl, $i_{applied}$ = 100 $\mu A/cm^2$, 10^6 cycles [64].

Figure 15. Schematic illustration of corrosion affected fatigue crack nucleation.

Figure 16. The effects of corrosion and pre-corrosion on the fatigue lives of a 7075-T6 alloy. Note that re-solutionizing and re-aging the alloy after precorrosion results in a significant increase in fatigue resistance.

Figure 17. Effect of cathodic polarization on the fatigue behavior of 7075 Al alloy in NaCl and Na_2SO_4.

Figure 18. Fatigue behavior of 7075 Al alloy in air and in aerated NaCl solution, (a) under Mode I loading, (b) under Mode 3 loading.

Figure 19. A schematic model of the effects of anodic and cathodic coatings on corrosion fatigue crack initiation.

Figure 20. Corrosion potentials and corrosion fatigue protection potentials for low carbon steel in NaCl+HCl as a function of pH. Note that the protection potential is independent of pH below the fatigue limit (in air) but not above the fatigue limit.

Figure 21. The effect of cathodic polarization on the fatigue behavior of 4140 steel (heat treated to R_c 52) in 3% NaCl solution at a stress level below the fatigue limit in air [99].

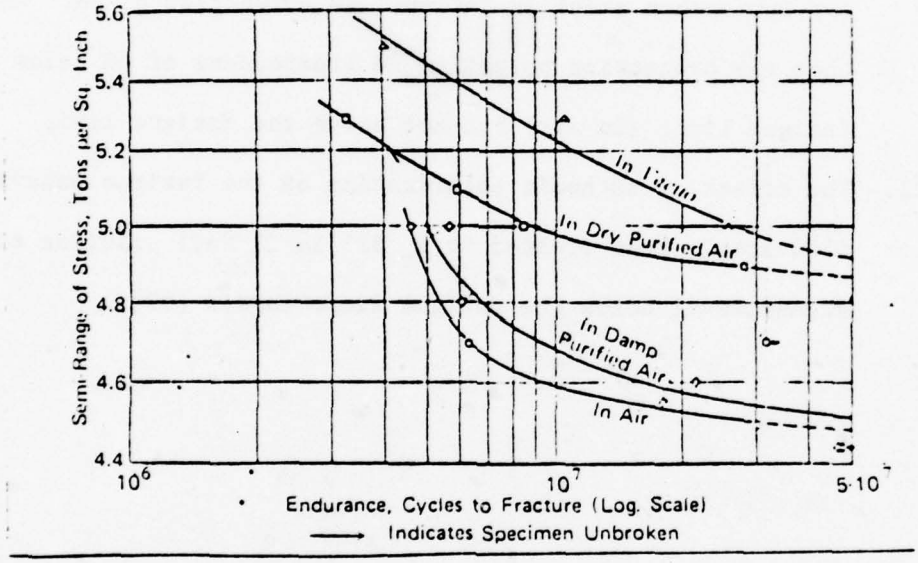

FIGURE 1. The effect of air and water vapor on the fatigue life of annealed copper [2].

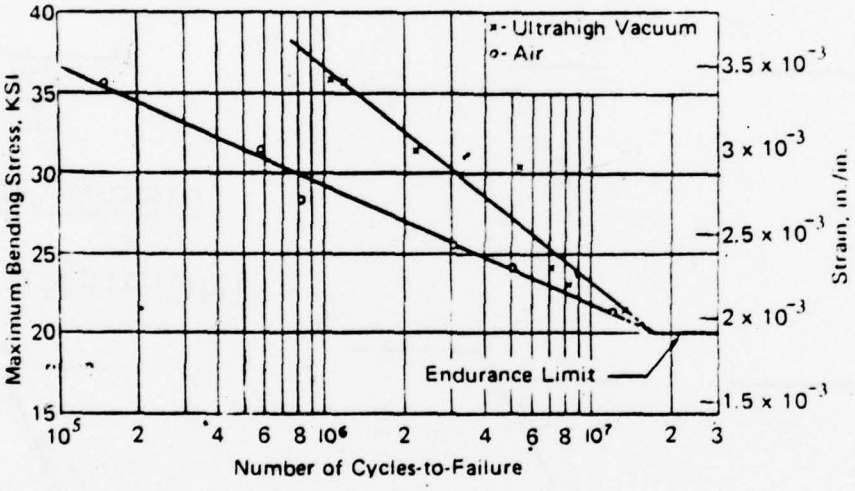

FIGURE 2. The effects of air versus vacuum on the fatigue life of a 2024-T3 Al alloy [18].

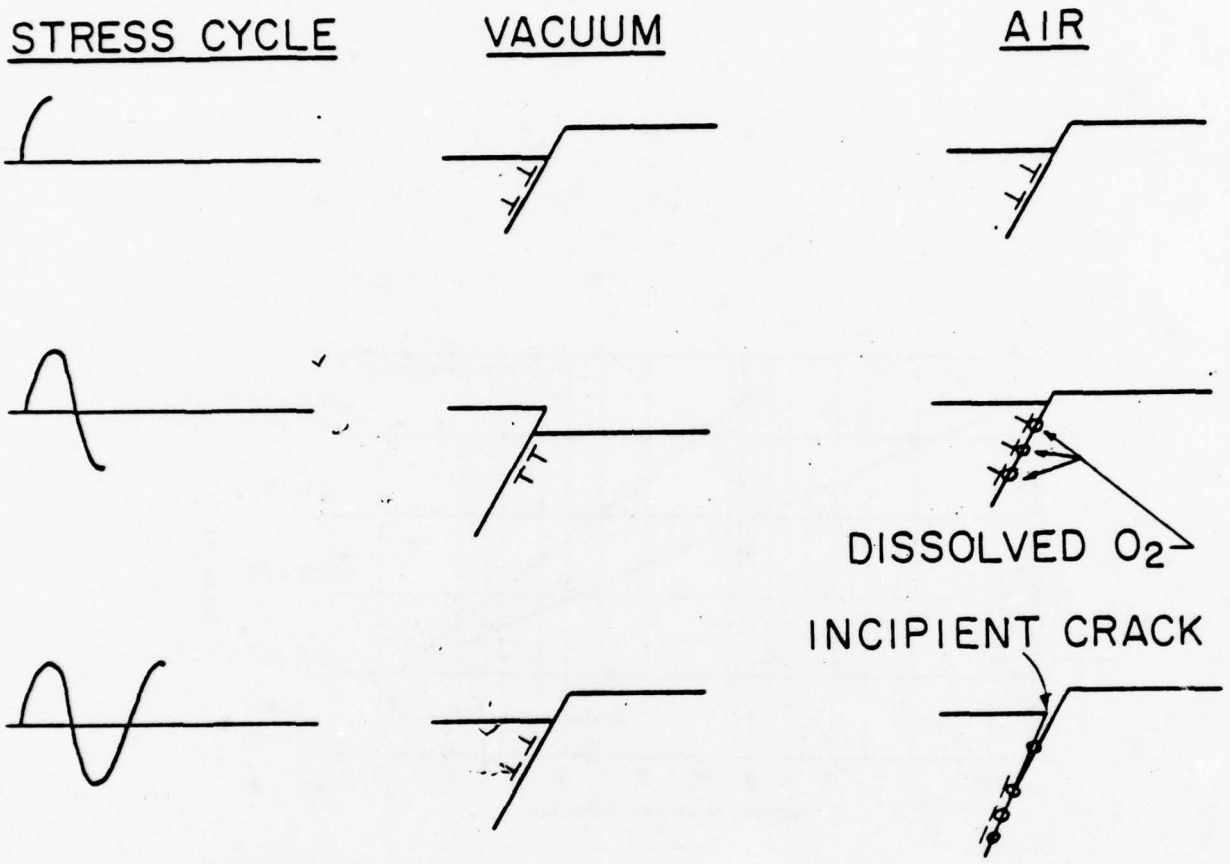

FIGURE 3. Model of oxygen/slip band interaction to explain environment sensitive fatigue crack nucleation [5].

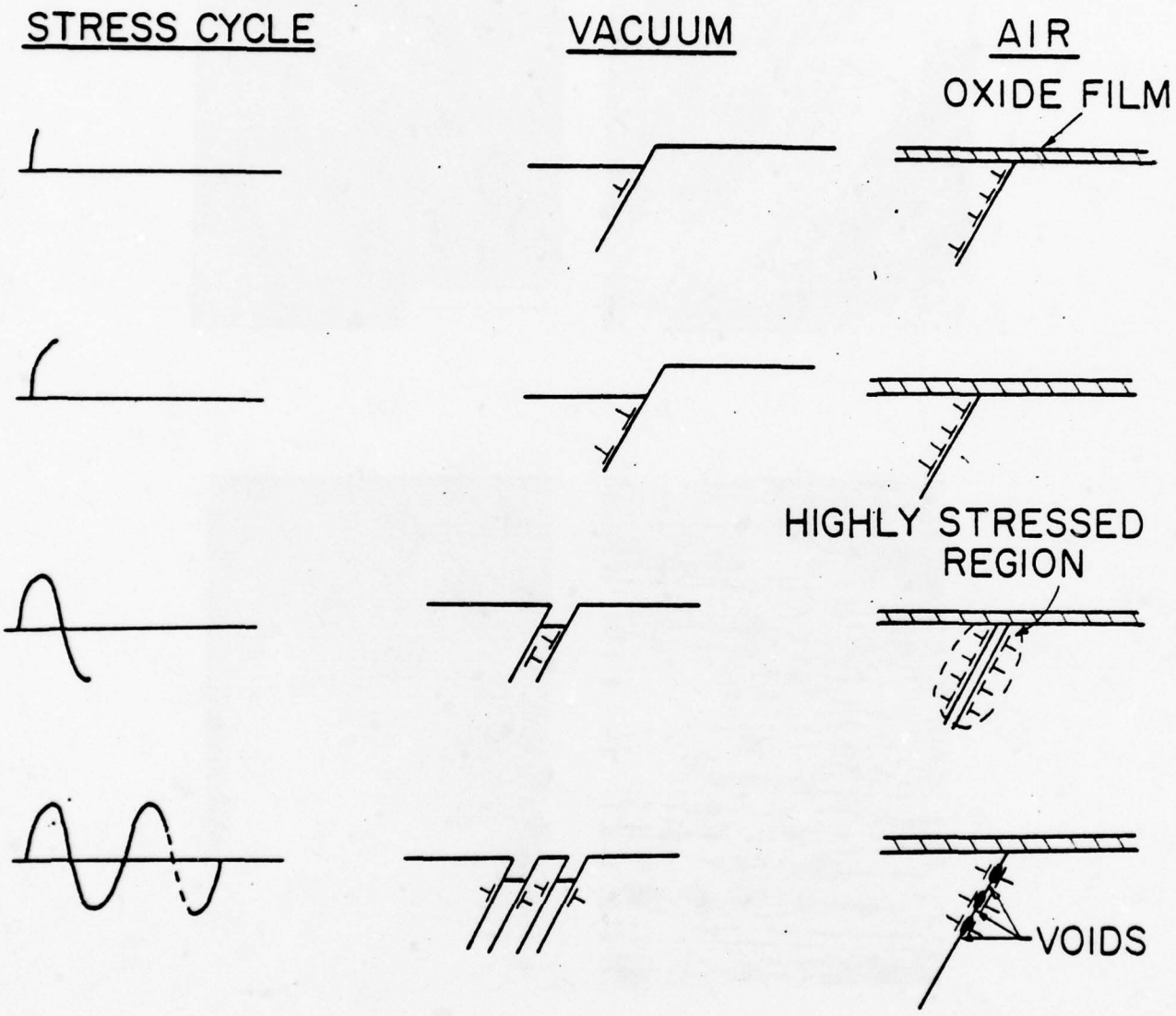

FIGURE 4. Model of void nucleation under oxide films to accelerate crack initiation in gaseous environments [19].

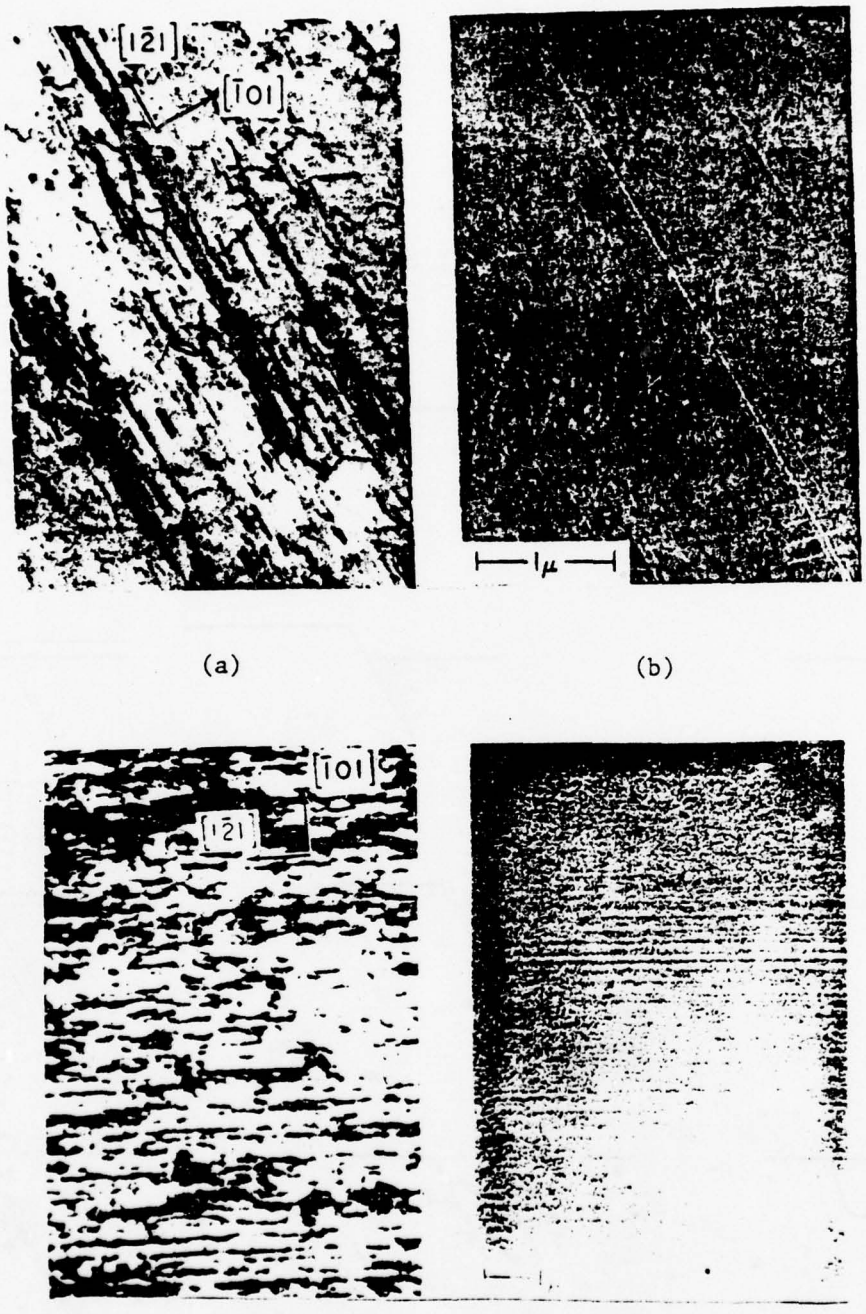

FIGURE 5. TEM micrograph of surfaces of cyclically deformed Al crystals. Figures 5a and 5b show the dislocation arrangements and resultant surface slip offsets observed in air and Figs. 5c and 5d show the results obtained in vacuum. Note that, in air surface slip offsets are more intense and dislocation arrangements more heterogeneous than in vacuum [26].

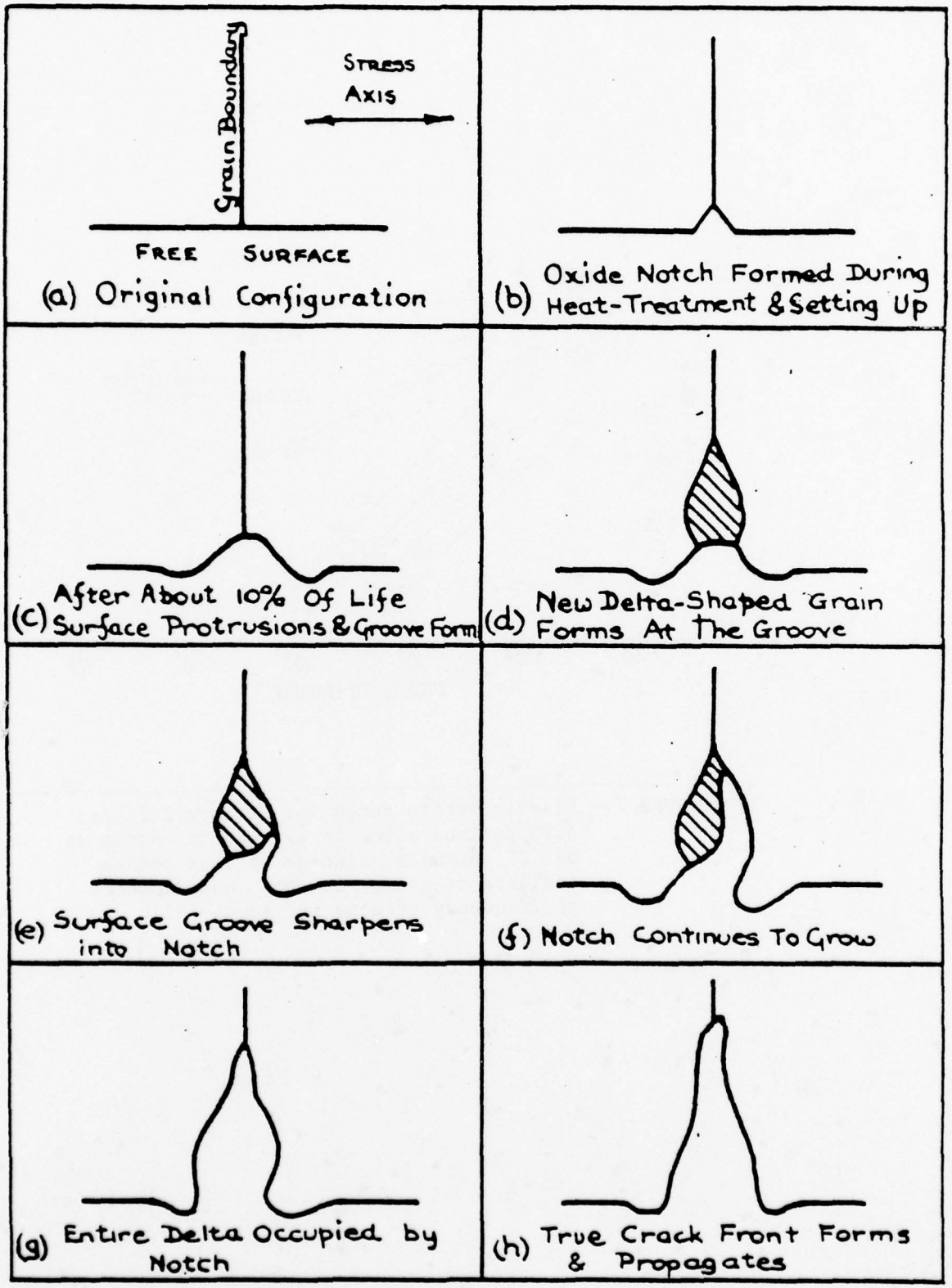

FIGURE 6. Model for fatigue crack nucleation in stainless steel at elevated temperature suggesting that an oxide created notch nucleates a new grain and subsequent crack nucleus [30].

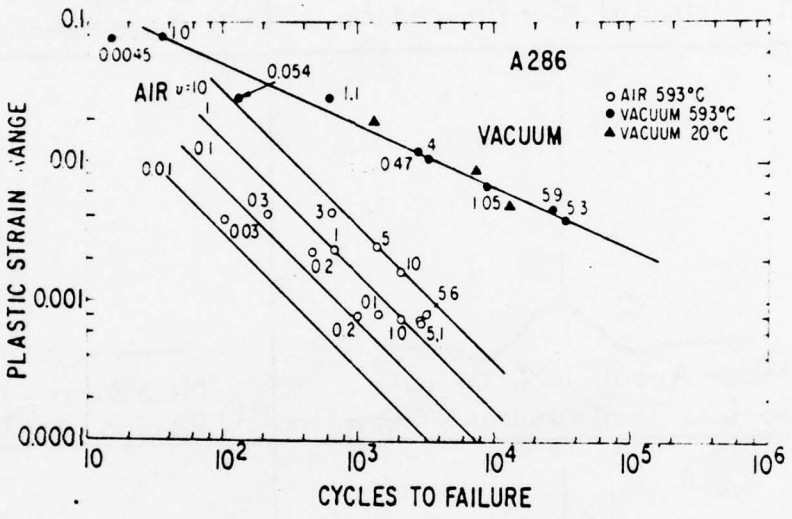

FIGURE 7. Plastic strain range vs. fatigue life for A286 ferrous alloy in air and in vacuum at 593°C. Numbers adjacent to test points indicate frequency in cpm. Note absence of frequency effects in vacuum [32].

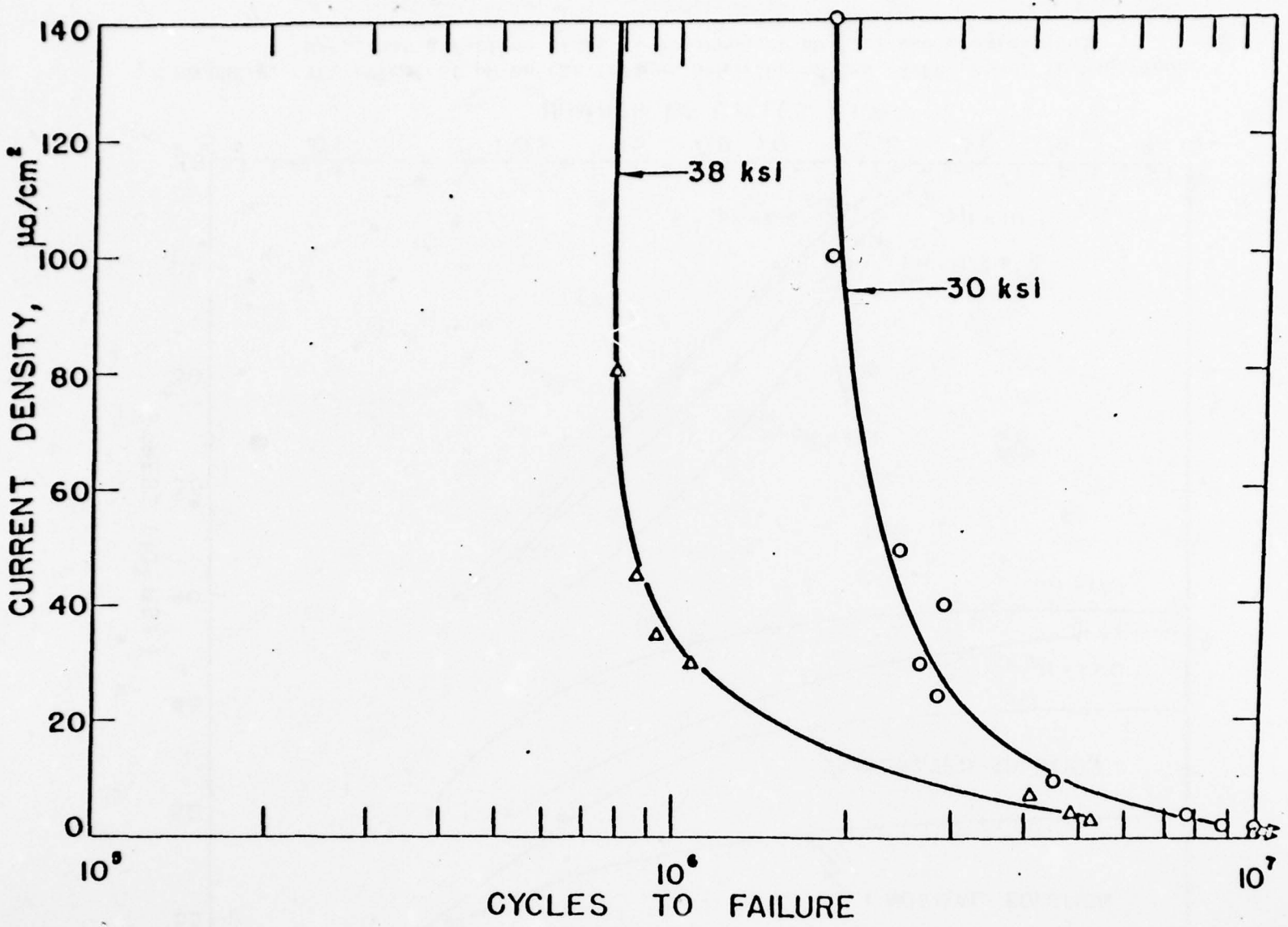

FIGURE 8. The effect of applied anodic currents on the fatigue lives of low carbon steel in deaerated 3% NaCl solution. The corrosion rate of the steel in this solution is virtually zero in the absence of applied currents. Note the independence of fatigue at currents greater than $\sim$ 40 $\mu A/cm^2$, the absence of an applied stress effect and the reappearance of a fatigue limit at currents less than $\sim$ 0.2 $\mu A/cm^2$ [42].

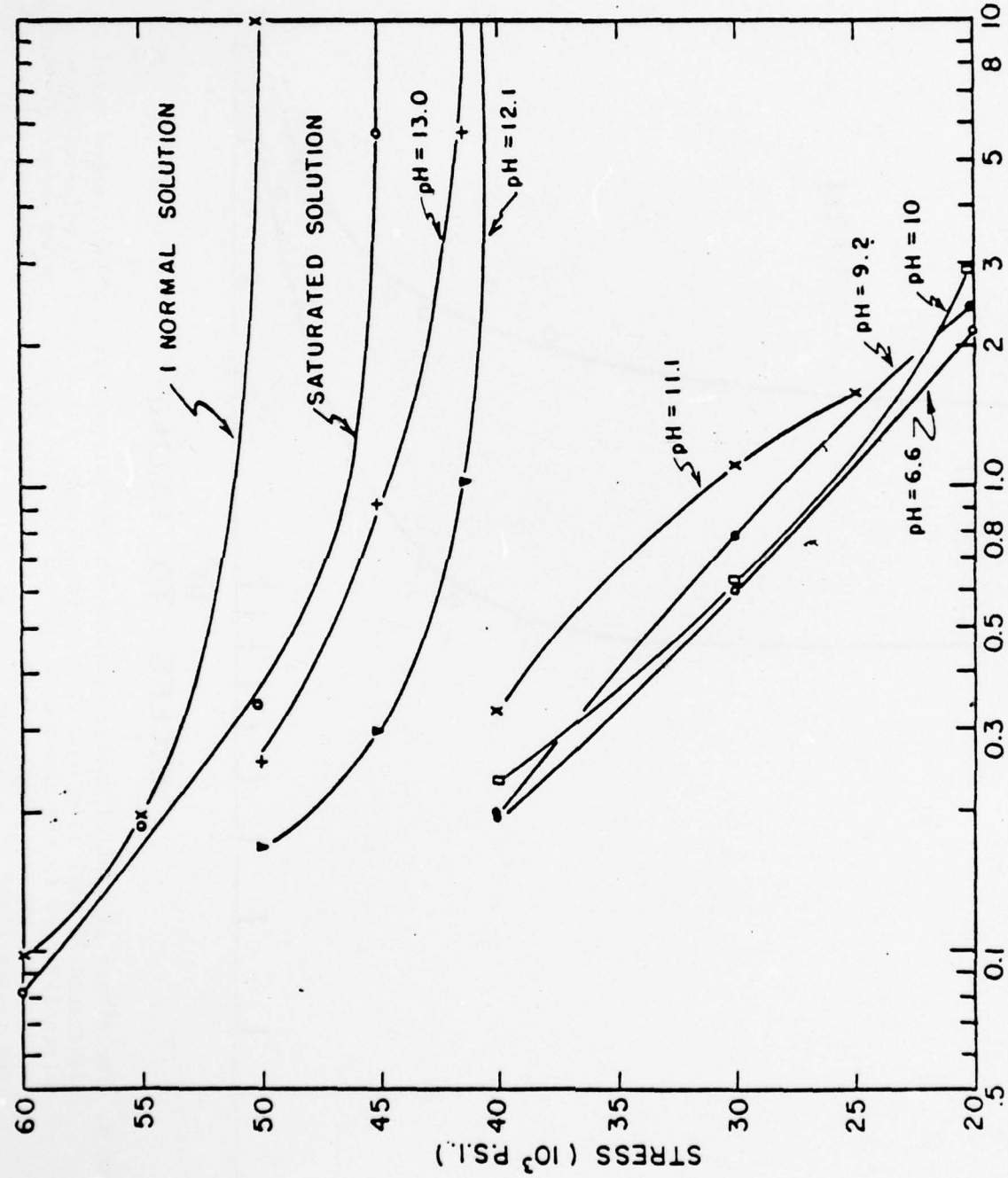

FIGURE 9. The effect of pH on the fatigue behavior of low carbon steel in NaCl+NaOH. Note that a fatigue limit is observed at pH 12.1 and greater [46].

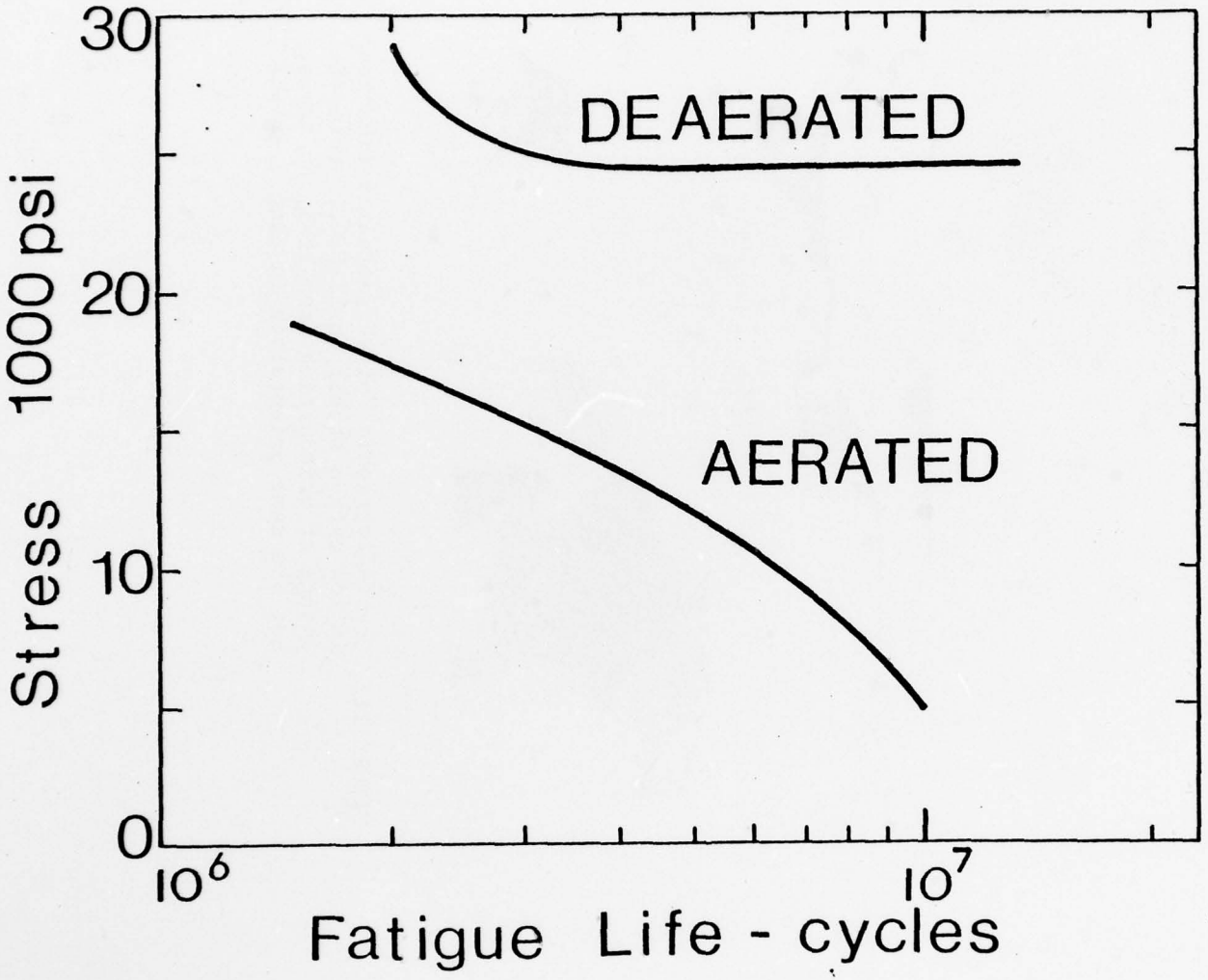

FIGURE 10. The effect of dissolved O_2 on the fatigue behavior of 1035 steel in 5% NaCl solution [54].

FIGURE 11. Crystallographic "pits" (actually trenches in low carbon steel) in 3% NaCl. Note the change of orientation from grain to grain, but the same orientation in single grains [55].

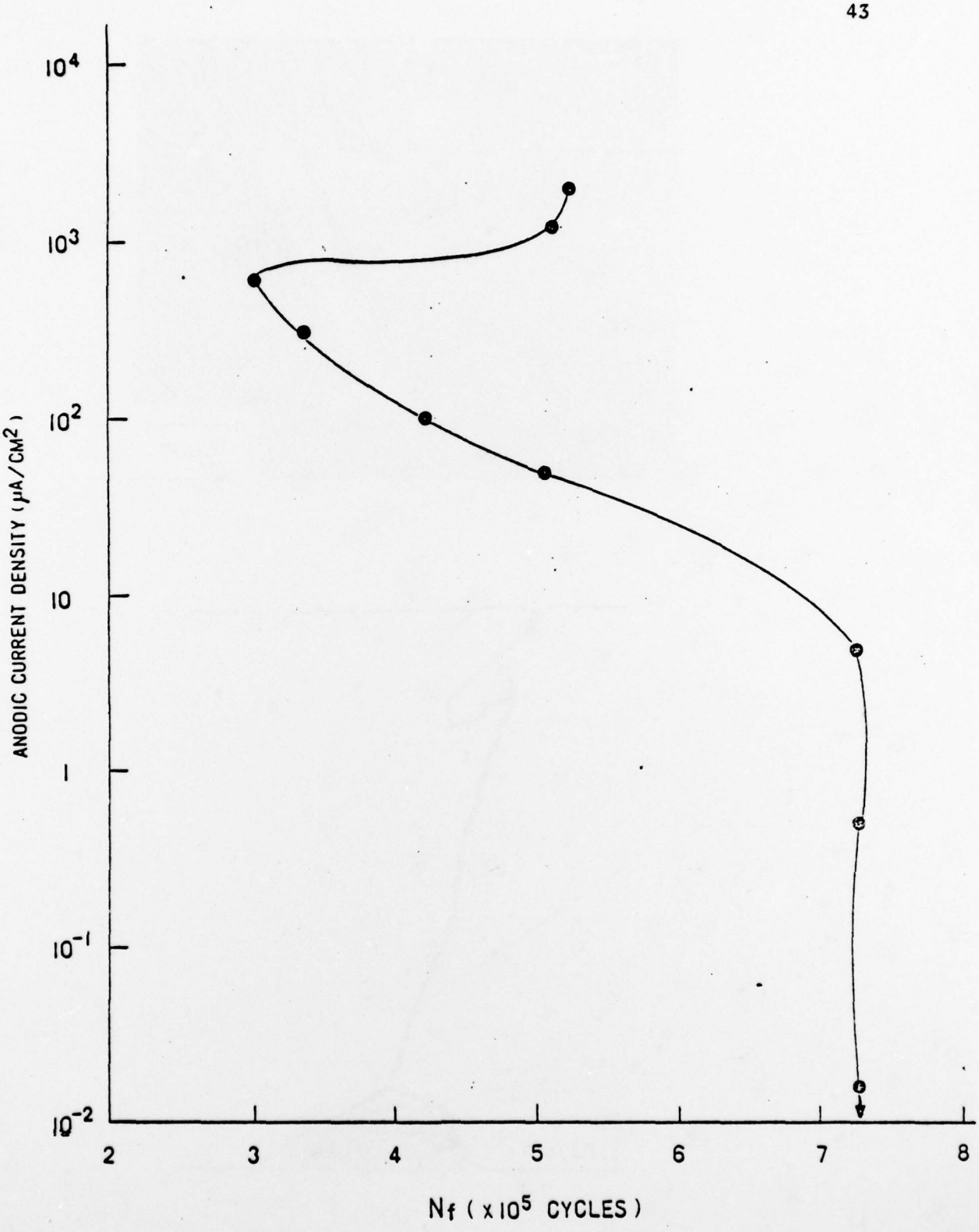

FIGURE 12. The effect of applied anodic current on the fatigue behavior of OFHC copper. Note the fatigue life independent region up to $\sim$ 10 $\mu A/cm^2$ and also the increase in fatigue life at currents greater than $\sim 10^3$ $\mu A/cm^2$ [56].

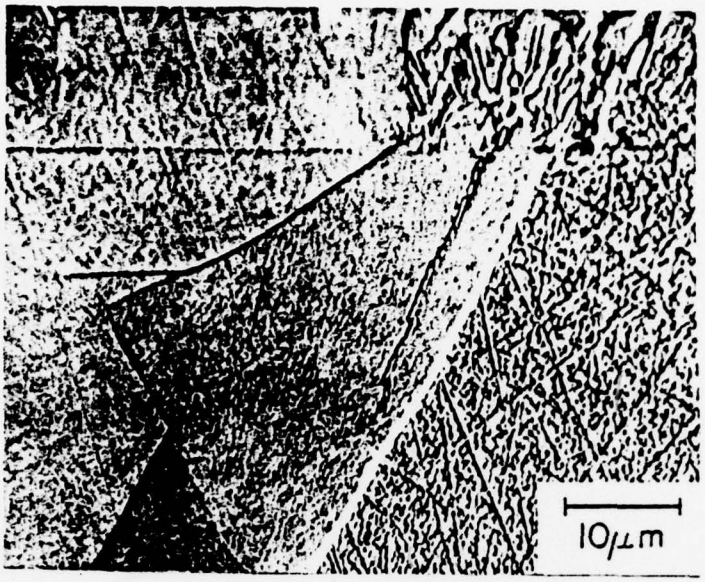

(a)

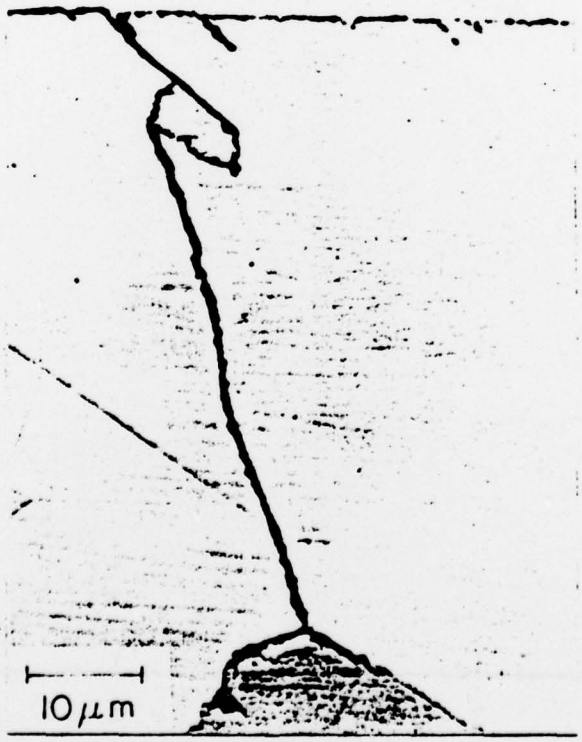

(b)

FIGURE 13. Longitudinal metallographic cross sections of Cu fatigued in (a) air showing transgranular cracking, and (b) in 0.5N NaCl showing mixed, but predominantly intergranular cracking.

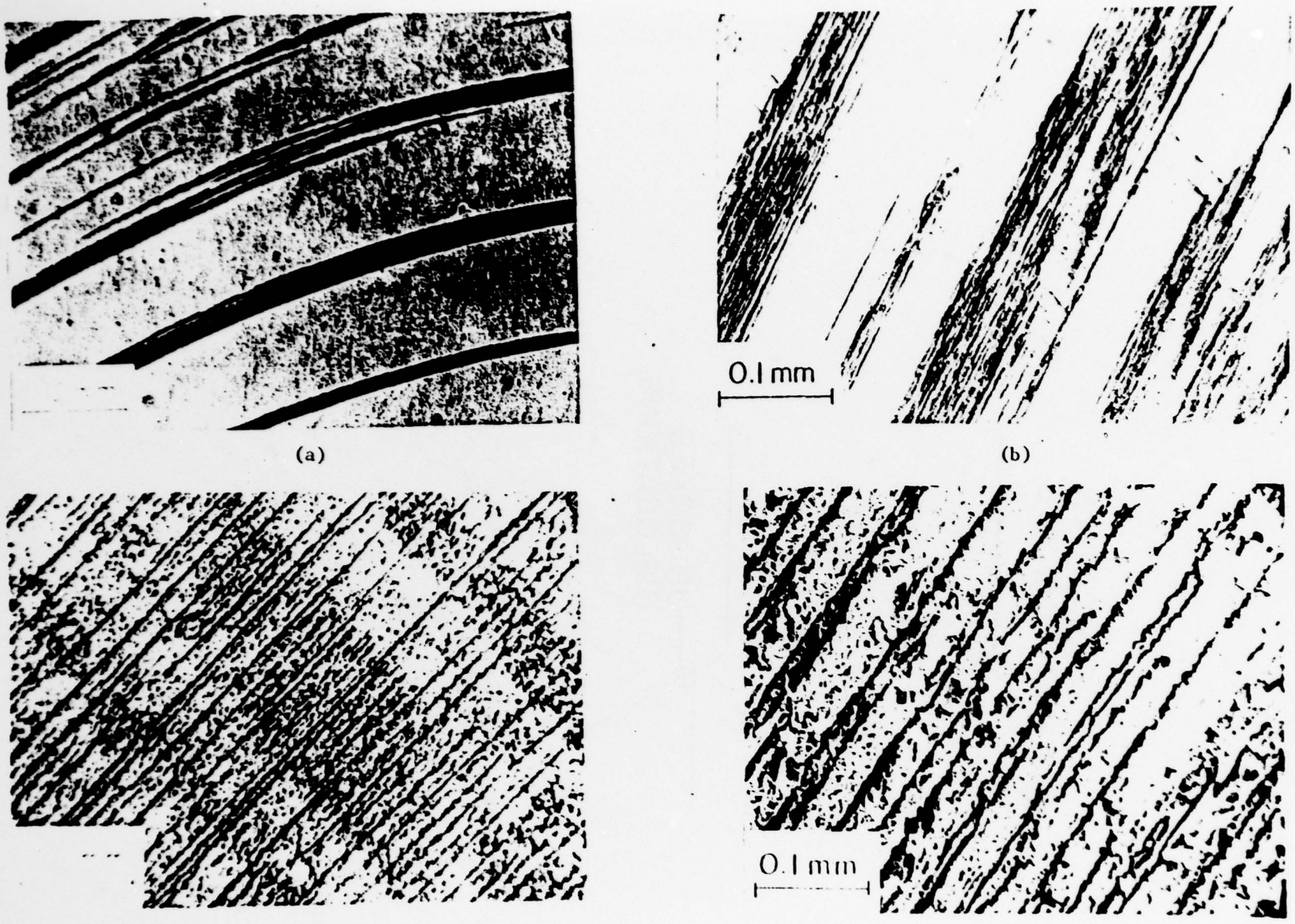

FIGURE 14. Copper single crystal surface slip offset appearance in (a) air, 10^5 cycles, (b) air, 10^6 cycles, (c) 0.5N NaCl, $i_{applied}$ = 100 μA/cm^2, 10^5 cycles, (d) 0.5N NaCl, $i_{applied}$ = 100 μA/cm^2, 10^6 cycles [64].

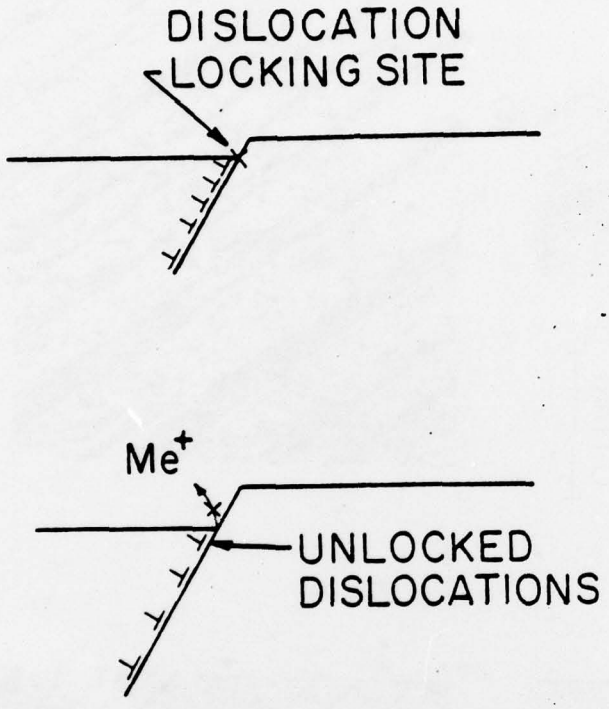

FIGURE 15. Schematic illustration of corrosion affected fatigue crack nucleation.

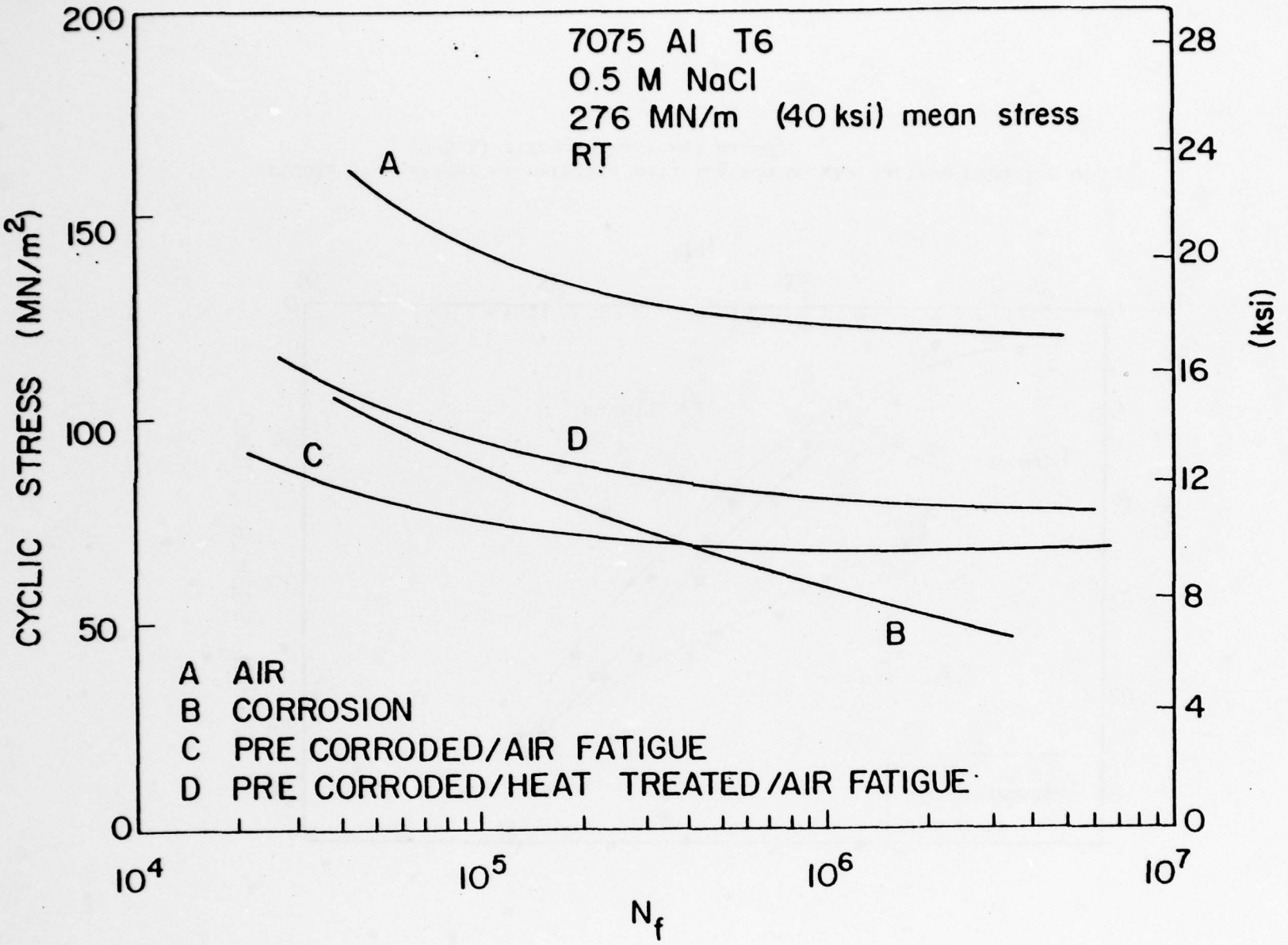

FIGURE 16. The effects of corrosion and pre-corrosion on the fatigue lives of a 7075-T6 alloy. Note that re-solutionizing and re-aging the alloy after precorrosion results in a significant increase in fatigue resistance.

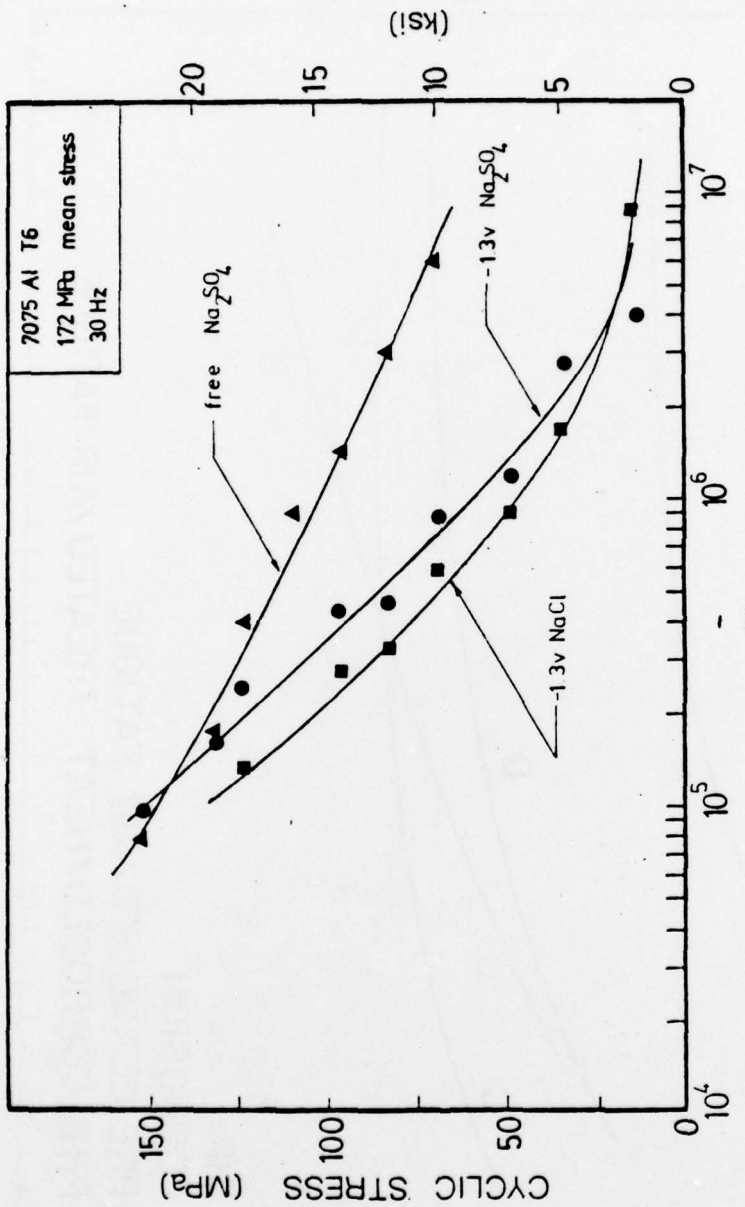

FIGURE 17. Effect of cathodic polarization on the fatigue behavior of 7075 Al alloy in NaCl and Na_2SO_4.

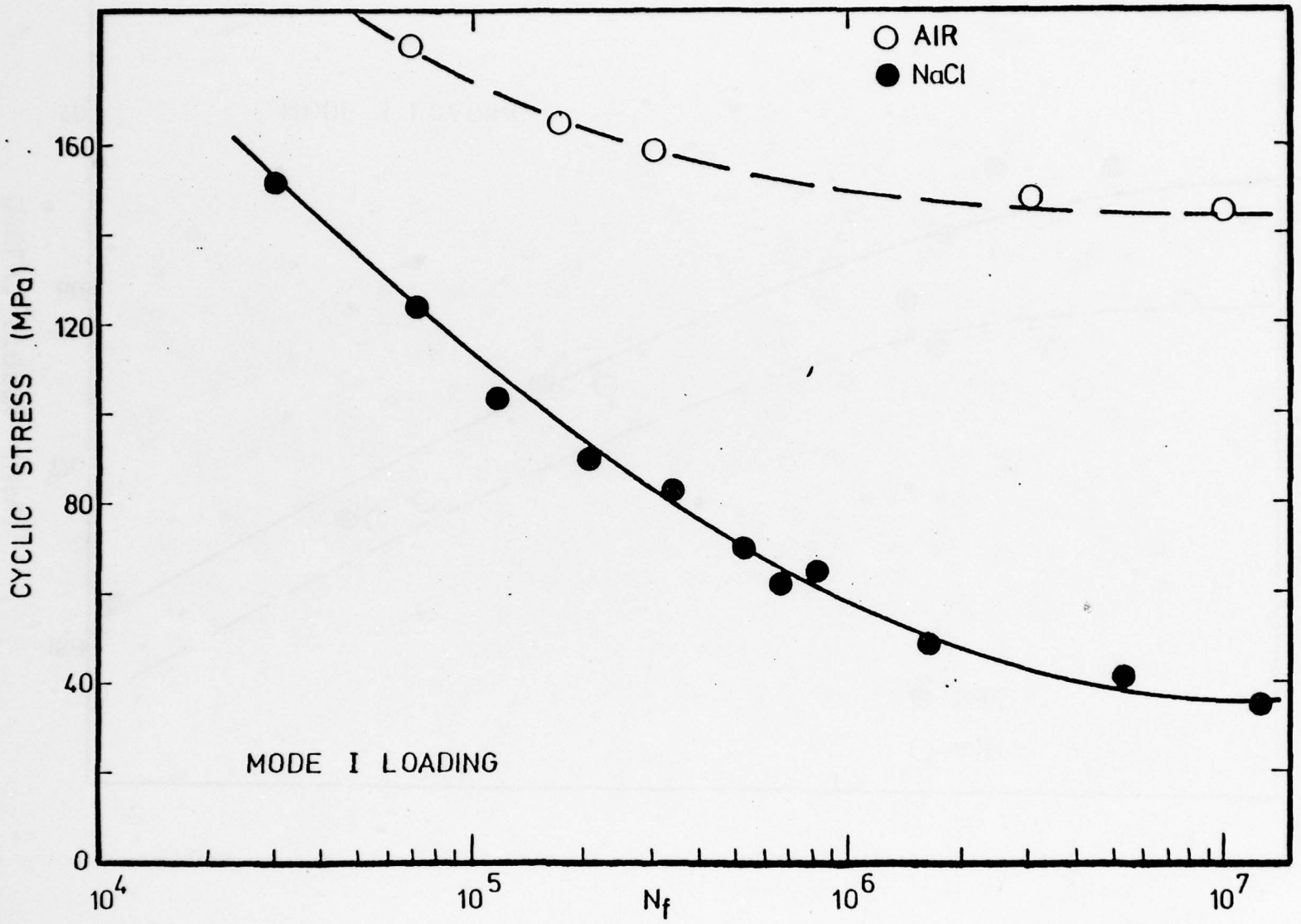

FIGURE 18a. Fatigue behavior of 7075 Al alloy in air and in aerated NaCl solution under Mode I loading.

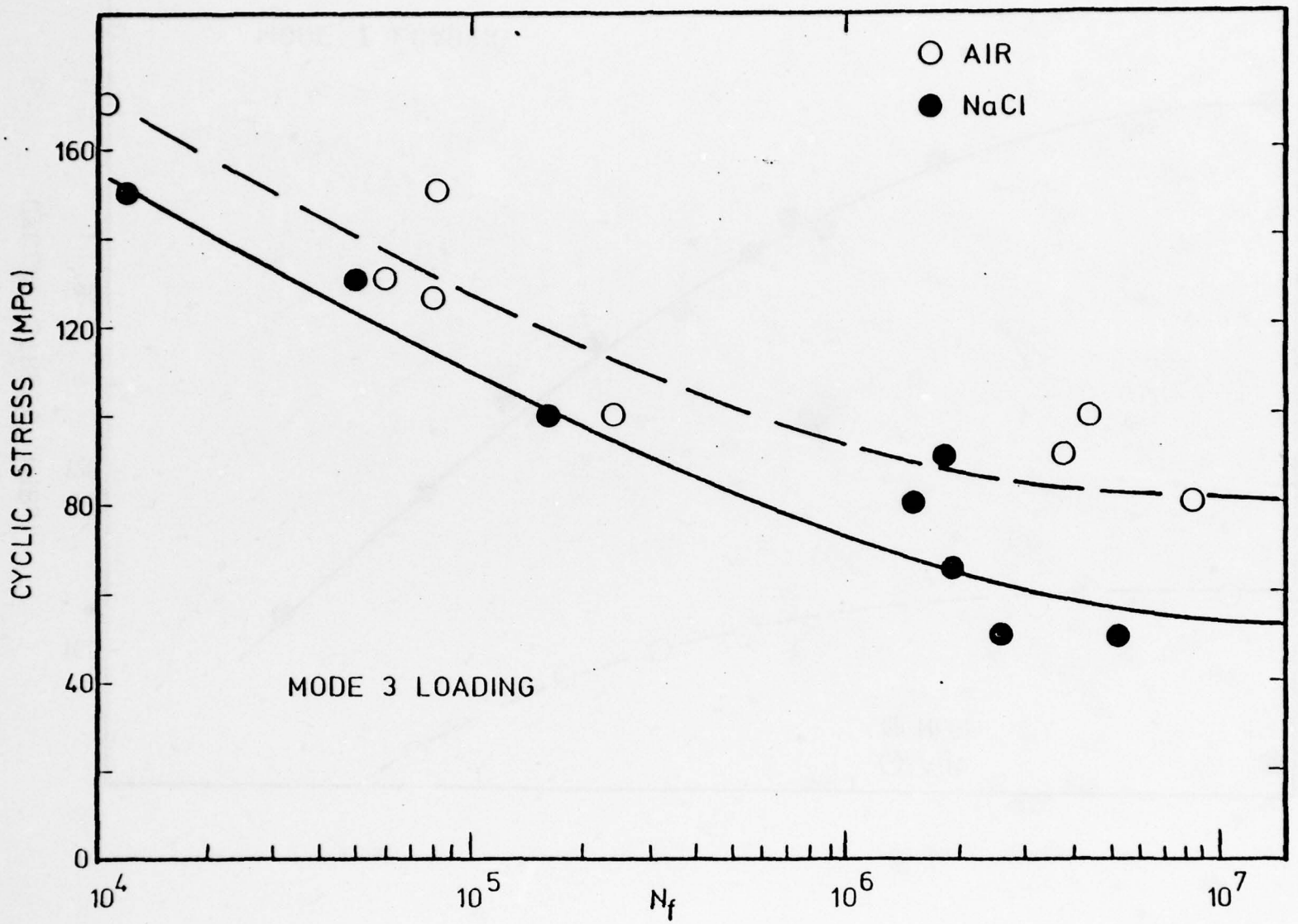

FIGURE 18b. Fatigue behavior of 7075 Al alloy in air and in aerated NaCl solution under Mode 3 loading.

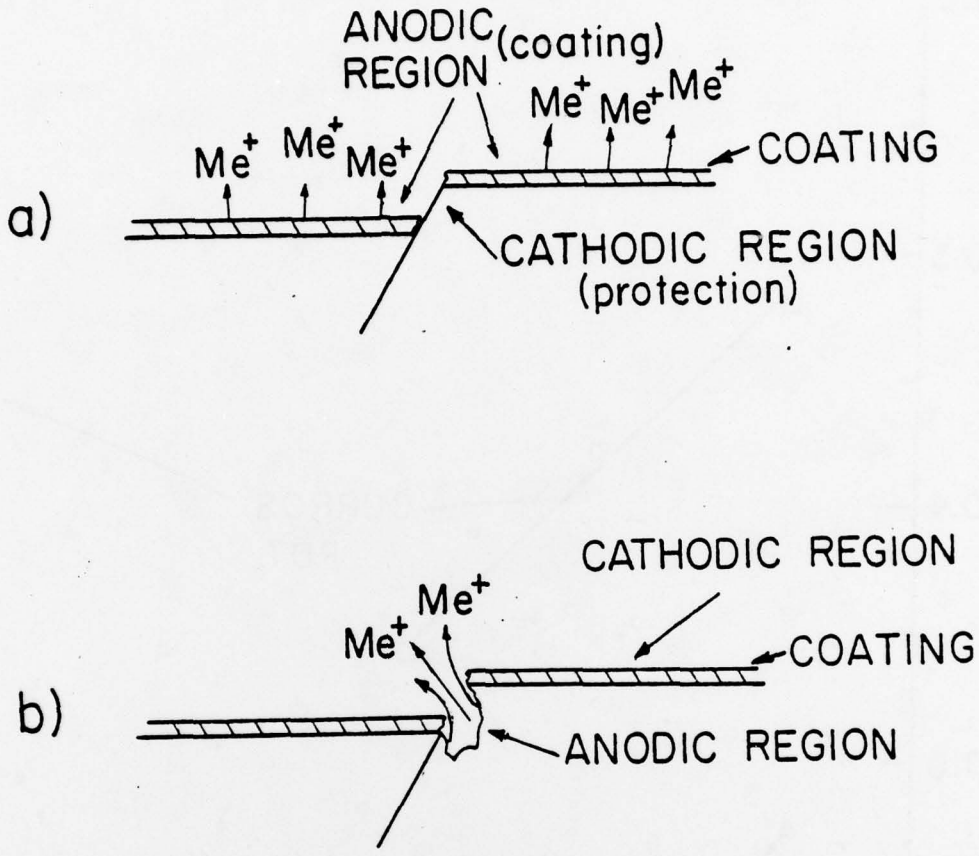

FIGURE 19. A schematic model of the effects of anodic and cathodic coatings on corrosion fatigue crack initiation.

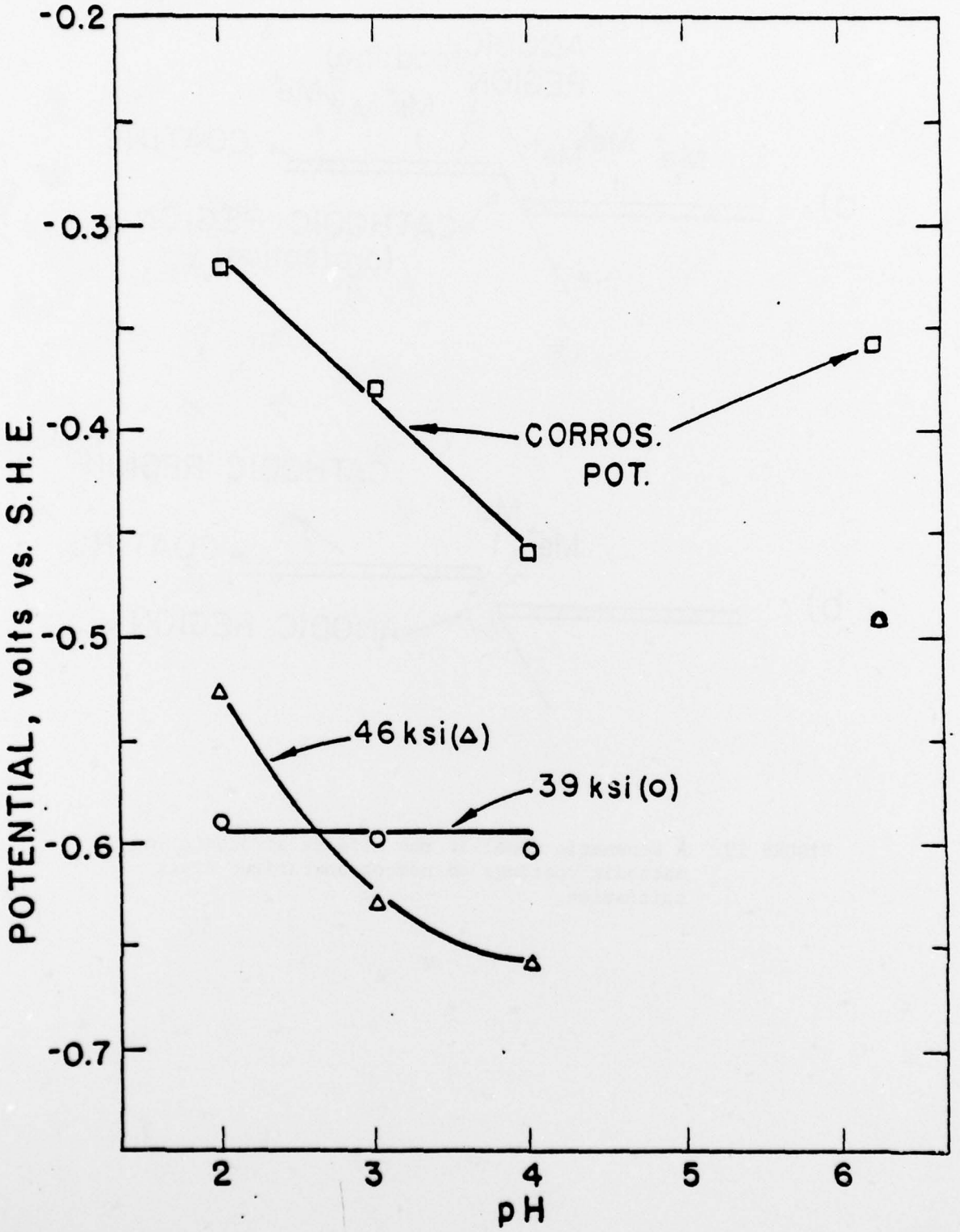

FIGURE 20. Corrosion potentials and corrosion fatigue protection potentials for low carbon steel in NaCl+HCl as a function of pH. Note that the protection potential is independent of pH below the fatigue limit (in air) but not above the fatigue limit.

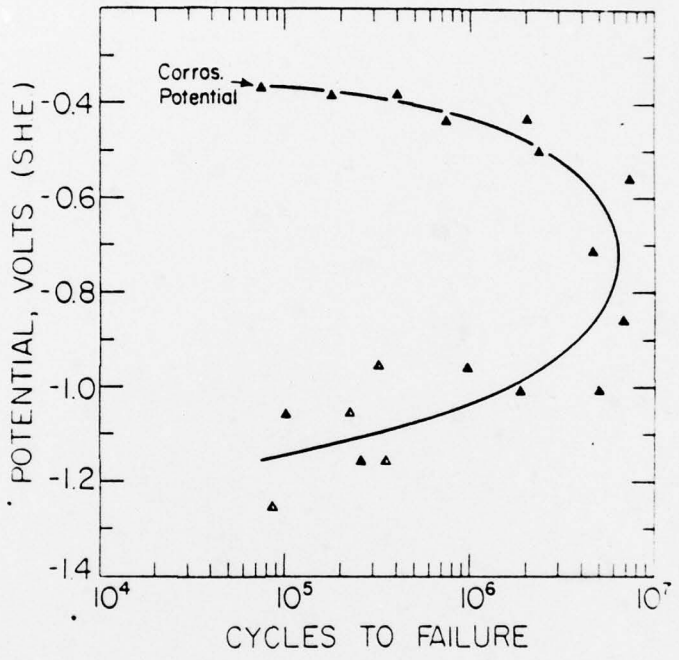

FIGURE 21. The effect of cathodic polarization on the fatigue behavior of 4140 steel (heat treated to R_c 52) in 3% NaCl solution at a stress level below the fatigue limit in air [99].

UNCLASSIFIED
Security Classification

DOCUMENT CONTROL DATA - R&D
(Security classification of title, body of abstract and indexing annotation must be entered when the overall report is classified)

1. ORIGINATING ACTIVITY (Corporate author) Rensselaer Polytechnic Institute Materials Engineering Department Troy, New York 12181	2a. REPORT SECURITY CLASSIFICATION Unclassified 2b. GROUP

3. REPORT TITLE
ENVIRONMENTAL EFFECTS ON GENERAL FATIGUE RESISTANCE AND CRACK NUCLEATION IN METALS AND ALLOYS

4. DESCRIPTIVE NOTES (Type of report and inclusive dates)
Technical Report

5. AUTHOR(S) (Last name, first name, initial)
Duquette, David J.

6. REPORT DATE	7a. TOTAL NO. OF PAGES	7b. NO. OF REFS
November 1978	53	99

8a. CONTRACT OR GRANT NO. b. PROJECT NO. N00014-75-C-0466 c. d.	9a. ORIGINATOR'S REPORT NUMBER(S) 9b. OTHER REPORT NO(S) (Any other numbers that may be assigned this report)

10. AVAILABILITY/LIMITATION NOTICES
Distribution of this document is unlimited

11. SUPPLEMENTARY NOTES	12. SPONSORING MILITARY ACTIVITY
	OFFICE OF NAVAL RESEARCH

13. ABSTRACT

The fatigue resistance of metals can be profoundly affected by environmental reactions which affect crack initiation and/or propagation. In the case of gaseous environments, oxide films or, in some cases, gas adsorption alone have been related to premature crack initiation for some materials. Crack initiation in other materials does not appear to be affected by gaseous environments, particularly at low temperatures, and there is not good agreement on the criteria which govern these phenomena.

In aqueous environments, on the other hand, virtually all corrosive environments affect crack initiation processes, sometimes by a simple phenomenon of pits acting as stress concentrators and, at other times, through what appears to be a far more complex phenomenon. This review details the general phenomena of the effects of environment on fatigue lives and discusses some of the current models which have been proposed to explain environmental effects on fatigue crack initiation.

DD FORM 1 JAN 64 1473

UNCLASSIFIED
Security Classification

14. KEY WORDS	LINK A		LINK B		LINK C	
	ROLE	WT	ROLE	WT	ROLE	WT
Fatigue Corrosion Fatigue Crack Initiation Environmental Effects						

INSTRUCTIONS

1. ORIGINATING ACTIVITY: Enter the name and address of the contractor, subcontractor, grantee, Department of Defense activity or other organization *(corporate author)* issuing the report.

2a. REPORT SECURITY CLASSIFICATION: Enter the overall security classification of the report. Indicate whether "Restricted Data" is included. Marking is to be in accordance with appropriate security regulations.

2b. GROUP: Automatic downgrading is specified in DoD Directive 5200.10 and Armed Forces Industrial Manual. Enter the group number. Also, when applicable, show that optional markings have been used for Group 3 and Group 4 as authorized.

3. REPORT TITLE: Enter the complete report title in all capital letters. Titles in all cases should be unclassified. If a meaningful title cannot be selected without classification, show title classification in all capitals in parenthesis immediately following the title.

4. DESCRIPTIVE NOTES: If appropriate, enter the type of report, e.g., interim, progress, summary, annual, or final. Give the inclusive dates when a specific reporting period is covered.

5. AUTHOR(S): Enter the name(s) of author(s) as shown on or in the report. Enter last name, first name, middle initial. If military, show rank and branch of service. The name of the principal author is an absolute minimum requirement.

6. REPORT DATE: Enter the date of the report as day, month, year; or month, year. If more than one date appears on the report, use date of publication.

7a. TOTAL NUMBER OF PAGES: The total page count should follow normal pagination procedures, i.e., enter the number of pages containing information.

7b. NUMBER OF REFERENCES: Enter the total number of references cited in the report.

8a. CONTRACT OR GRANT NUMBER: If appropriate, enter the applicable number of the contract or grant under which the report was written.

8b, 8c, & 8d. PROJECT NUMBER: Enter the appropriate military department identification, such as project number, subproject number, system numbers, task number, etc.

9a. ORIGINATOR'S REPORT NUMBER(S): Enter the official report number by which the document will be identified and controlled by the originating activity. This number must be unique to this report.

9b. OTHER REPORT NUMBER(S): If the report has been assigned any other report numbers *(either by the originator or by the sponsor)*, also enter this number(s).

10. AVAILABILITY/LIMITATION NOTICES: Enter any limitations on further dissemination of the report, other than those imposed by security classification, using standard statements such as:

(1) "Qualified requesters may obtain copies of this report from DDC."

(2) "Foreign announcement and dissemination of this report by DDC is not authorized."

(3) "U. S. Government agencies may obtain copies of this report directly from DDC. Other qualified DDC users shall request through _____."

(4) "U. S. military agencies may obtain copies of this report directly from DDC. Other qualified users shall request through _____."

(5) "All distribution of this report is controlled. Qualified DDC users shall request through _____."

If the report has been furnished to the Office of Technical Services, Department of Commerce, for sale to the public, indicate this fact and enter the price, if known.

11. SUPPLEMENTARY NOTES: Use for additional explanatory notes.

12. SPONSORING MILITARY ACTIVITY: Enter the name of the departmental project office or laboratory sponsoring *(paying for)* the research and development. Include address.

13. ABSTRACT: Enter an abstract giving a brief and factual summary of the document indicative of the report, even though it may also appear elsewhere in the body of the technical report. If additional space is required, a continuation sheet shall be attached.

It is highly desirable that the abstract of classified reports be unclassified. Each paragraph of the abstract shall end with an indication of the military security classification of the information in the paragraph, represented as *(TS)*, *(S)*, *(C)*, or *(U)*.

There is no limitation on the length of the abstract. However, the suggested length is from 150 to 225 words.

14. KEY WORDS: Key words are technically meaningful terms or short phrases that characterize a report and may be used as index entries for cataloging the report. Key words must be selected so that no security classification is required. Identifiers, such as equipment model designation, trade name, military project code name, geographic location, may be used as key words but will be followed by an indication of technical context. The assignment of links, rules, and weights is optional.